Energy Conversion and Management 171 (2018) 1365–1387

Contents lists available at ScienceDirect

Energy Conversion and Management

journal homepage: www.elsevier.com/locate/enconman

Review

Technological challenges and optimization efforts of the Stirling machine: A review

Houda Hachem[a,*], Ramla Gheith[a], Fethi Aloui[b], Sassi Ben Nasrallah[a]

[a] Université de Monastir, École Nationale d'Ingénieurs de Monastir, Laboratoire LESTE, Avenue Ibn El Jazzar 5019 Monastir, Tunisia
[b] University of Lille North of France – University of Valenciennes (UVHC), LAMIH CNRS UMR 8201, Department of Mechanics, Campus Mont Houy, 59313 Valenciennes Cedex 9, France

ARTICLE INFO

Keywords:
Challenge
Modeling and optimization
Applications
Stirling machine

ABSTRACT

The Stirling engines are being carried out worldwide, used for divers' application such as solar generator, micro cogeneration and cryogenic uses. The present paper is an over view of Stirling technologies researches. Several possibilities of resolving technical challenges encountered when manufacturing or using Stirling machines will be discussed. The most appropriate models and optimizations strategies are reported. Stirling engine performances are derived as function of geometric parameters (swept volumes, dead volumes, heat exchange areas, compression ratio…) for several working conditions (speed, mean pressure, temperature difference and working fluid). The effect of each parameter on the Stirling performances when using numerical and/or experimental approaches are presented. It is concluded that multi-objective optimizations methods are useful for predicting geometric and working parameters that corresponding to the optimal performances of the Stirling engine.

1. Introduction

The increasing awareness of the limitation of the world's energy resources has sparked the interest of scientifics to develop new techniques to better use and valorize the existing resources. This situation has encouraged the improvement of energy efficiency, the development of renewable energies, the valorization of thermal discharges, the development of cogeneration or tri-generation systems and the hybridization of different energy sources. In this context, Stirling technology, which could contribute to the future energy mix, benefits from its many advantages over internal combustion engines. The Stirling engine was invented in 1816 by Scottish pastor Robert Stirling [1], before the Diesel engine (1893), the petrol engine (1860) and the electric motor (1869). The study of Stirling technologies has started from 1816 and continued to be improved until today.

The N. V. Philips society of The Netherlands was the first great society interested by Stirling engine since 1936 [2] thanks to its undeniable advantages in stationary operation. It is characterized by a silent mode of operation. It produces little vibration compared to the internal combustion engine. Thanks to the absence of the explosion, the absence of the valves that open and close, the absence of gas escaping, the Stirling engine requires easy maintenance. These engines are robust and deteriorate less rapidly than internal combustion engines. Unlike the internal combustion engine, Stirling engines fits with any heat source, not only conventional solid fuels, liquid or gaseous, by simple adaptation of the burner, but also heat recovered on other systems, the heat of nuclear or solar origin, etc … In this area, great progress can be made when coupling high heat loss systems with a system that can value these losses. Many Stirling engines are manufactured and used for various applications. Table 1 describes working conditions and performances of different types of old high power Stirling engines.

The original goal is to use the Stirling machine as an engine. However, the first real industrial application of this engine uses the reverse cycle to produce cold [8]. Most of the industrial applications of the Stirling cycle concern the refrigeration applications, in particular in cryogenics, where the Stirling cycle presents enormous advantages [8]. It is possible to reach low temperatures quickly, which increases its competitiveness compared to other refrigerating machines. In 1834, John Herschel designed a cooling machine using closed-cycle air for ice manufacture. Philips society developed also refrigeration machines and heat pumps based on the reverse Stirling cycle. In 1941, Philips built a cooler reaching −40 °C. Later, in 1945, Philips made a cooler reaching −200 °C using hydrogen as a working fluid. Between1960 and 1970, Philips sold an industrial Stirling chiller with a cooling capacity of 25 kW to 77 kW. Such machines require an input of mechanical work to accomplish their operation [1]. The Stirling cycle is fundamentally different from the Rankine cycle used in conventional refrigerators [9]. Unlike the Rankine cycle, the working fluid within the Stirling cycle

* Corresponding author.
E-mail address: houdahachem@yahoo.fr (H. Hachem).

https://doi.org/10.1016/j.enconman.2018.06.042
Received 6 March 2018; Received in revised form 23 May 2018; Accepted 12 June 2018

Table 1
Working conditions and performances of old high power Stirling Engines.

Stirling engine type designation	Working conditions					Performances		Cylinder dimensions			Ref(s)
	Speed (rpm)	Mean pressure (bar)	Working gas	Mean hot space temperature (°C)	Mean cold space temperature (°C)	Mechanical output power (KW)	Thermal efficiency (%)	Bore (mm)	Stroke (mm)	Number of cylinders	
Double acting SE developed by MAN	1000	150	He	760		225		–	–	6	[3]
Double acting SE	1010	50	He	747		35		142	76	4	[4]
The NASA 25 kWe FPSE		100	He	800		25				1	[5]
Sunpower RE-1000 FPSE	1800	70	He	541	49	1		57.22	40	1	[6]
Sunpower M100 FPSE		22		593	49			–	–	1	
Ford 4-215	4500	200	H_2	750	64	200		73	52	4	[7]
GPU3 General motors	2500	69	H_2	704	15	7.5		69.9	70.1	1	[7]
SE Prototype developed by United Stirling	2000	145	H_2	691	71	35	30	–	–	4	[2]
4-235 SE Prototype developed by Philips	1800	221	He	683	43	175	31	–	–	4	[2]
40 HP SE Prototype developed by Philips	725	142	H_2	649	16	23	38	–	–	4	[2]
Anal. Ph. 1 SE developed by United Stirling	1200	145	H_2	719	71	76	35	–	–	8	[2]
4-400 SE developed by Man-MWH	1000	108	He	633	41	88	32	–	–	4	[2]

undergoes no phase change. The Stirling cycle cryocoolers is widely used because of its advantages: high efficiency, fast cool-down, small size, light weight, low power consumption, high reliability, no pollutant generation like carbon monoxide and so on [10]. Nowadays, the Stirling cycle cryocooler is applied to domestic and commercial refrigerators. Table 2 describes performances and working conditions of old Stirling cryocoolers.

In this article, we present over view of Stirling technologies researches. Section 2 presents an overview of Stirling technology. Section 3 describes the Stirling engine applications. Section 4 presents technological challenges uncounted during manufacture and use of Stirling engines. Section 5 presents models and different optimizations methods made to enhance the performances of these machines. Optimization criterion, methods and parameters used will be investigated. Finally, conclusions are summarized in Section 6.

2. Over view of the Stirling technology

2.1. Cycle and main operation

The Stirling engine (SE) uses a working fluid (air, helium, hydrogen …) contained in a closed domain. Heated by an external hot source at one end and cooled by an external cold source at the other end. The pressure of the working gas will increase on heating and decrease on cooling. Repeated heating and cooling will cause a reciprocating movement of the piston which can be converted to rotary motion using a mechanical drive system. The gas inside the SE is moving from the hot side to the cold side and it is alternately expanding and contracting. The piston movement is converted into useful mechanical work.

The Stirling cycle is a reversible one. It means that inassimilable phenomena can arrive from an engine designed according to this cycle [8]. Providing a temperature difference to this engine leads to get a mechanical power output. In this case the Stirling machine is called heat engine (Fig. 1(a)). But, conversely, bring mechanical energy to the same engine, leads to produce cold or hot heat quantities. In this case the Stirling machine is called a heat pump or cooler depending on the direction of rotation (Fig. 1(b)) [12].

The Stirling's ideal thermodynamic cycle is composed of two isochoric and two isotherms. It is similar to the Carnot cycle; the only difference between them is that the two isothermal processes in the Carnot cycle are replaced by two isochoric processes in the Stirling cycle. As shown in Fig. 2, the working gas trapped in the engine undergoes the following transformation: During the first transformation ($3 \rightarrow 4$), the volume of the gas decreases and the pressure increases as it gives up heat Q_k to the cold source. During the second transformation ($4 \rightarrow 1$), the volume of the gas remains constant as it passes back through the regenerator and regains some of its previous heat. During the third transformation (12)→, the gas absorbs energy Q_h from the hot source, its volume increases and its pressure decreases, while the temperature remains constant. Finally, during the fourth and last transformation ($2 \rightarrow 3$), the volume of the gas remains constant as it transfers through the regenerator and cools. Compared to Ericsson engine, at nearly the same working conditions, the Stirling engine presents higher specific indicated work and efficiency due to the presence of the regenerator [11].

The actual efficiency of Stirling engines is obviously lower than the theoretical efficiency. The first reason is that heat transfer requires keeping a temperature difference between the sources and the working fluid. Thus, in particular, the internal transfer only partially supports heating 4-1 and cooling 2-3. We denote by α the fraction of heat exchanged:

$$q_{4a} = \alpha q_{41} = -q_{2b} = -\alpha q_{23} \quad (1)$$

The rest heat exchanged quantities q_{a1} and q_{b3}, must be performed with sources and significant thermal differences, which consumes extra energy at the hot source (q_{a1}), increases irreversibilities, and therefore

Table 2
Working conditions and performances of old Stirling cryocoolers [171]

Stirling cryocooler type designation	Refrigerating capacity (kW)		Power input (kW)		Working conditions		Dimensions			
	At 110 K	At 80 K	At 110 K	At 80 K	Speed (rpm)	Mean pressure (bar)	Piston diameter (cm)	Piston stroke (cm)	Numbers of cylinders	Working fluid
Philips PPG102	1.5	1	7	9	1450	25	7	5.3	1	He
Philips PPG400	6	4	28	36	1450	25	–	–	4	H_2
Philips PPG2500	44	25	160	180	730	40	17.5	9.3	4	–
Werksper CGR	13	11	62	75	1500	35	26	3.27	1	–

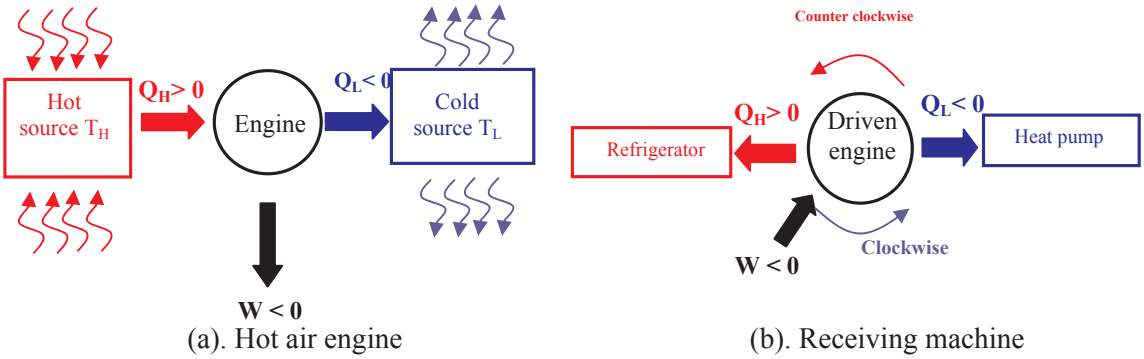

Fig. 1. Operation principe of Stirling engine.

decreases the efficiency.

The second reason is that, despite the technological efforts made, transfers 1-2 and 3-4 with sources are never isothermal and transformations 4-1 and 2-3 do not strictly correspond to polytropes. All transformations have a certain level of irreversibility.

In the Stirling cycle (Fig. 2) the thermal exchanges with sources also correspond to transformations with mechanical energy exchange, since, being isochoric, the two other transformations take place without work: $W_{41} = W_{23} = 0$. We can therefore write, considering the law of perfect gases P V = r T:

$$W_{12} = -rT_{max}ln\varepsilon \quad and \quad W_{34} = rT_{min}ln\varepsilon \tag{2}$$

$$W = W_{12} + W_{34} = rln\varepsilon(T_m - T_M) \tag{3}$$

With ε is the volumetric compression ratio:

$$\varepsilon = \frac{V_2}{V_1} = \frac{V_3}{V_4} \tag{4}$$

The temperature and the internal energy being constant, the amount of heat received from the hot source is:

$$q_{max} = q_{12} = -W_{12} = rT_{max}ln\varepsilon \tag{5}$$

Let us examine the influence of thermal gradients in exchanges (Fig. 2) on the yield and, firstly, that of the coefficient α. In this case, the expression of the job does not change. On the other hand, the heat that hot source must supply is increased by the quantity $(1 - \alpha)$. q_{41}. As:

$$q_{41} = \Delta u_{41} = c_v(T_{max} - T_{min}) = \frac{r}{\gamma - 1}(T_{max} - T_{min}) \tag{6}$$

Thermal efficiency of the Stirling cycle is expressed as:

$$\eta_{th} = -\frac{W}{q_M + (1-\alpha)q_{41}} = \eta_c \frac{1}{1 + \frac{1-\alpha}{\gamma - 1}\frac{\eta_c}{ln\varepsilon}} \tag{7}$$

With η_{th} is the Carnot yield calculated with the extreme temperatures of the cycle.

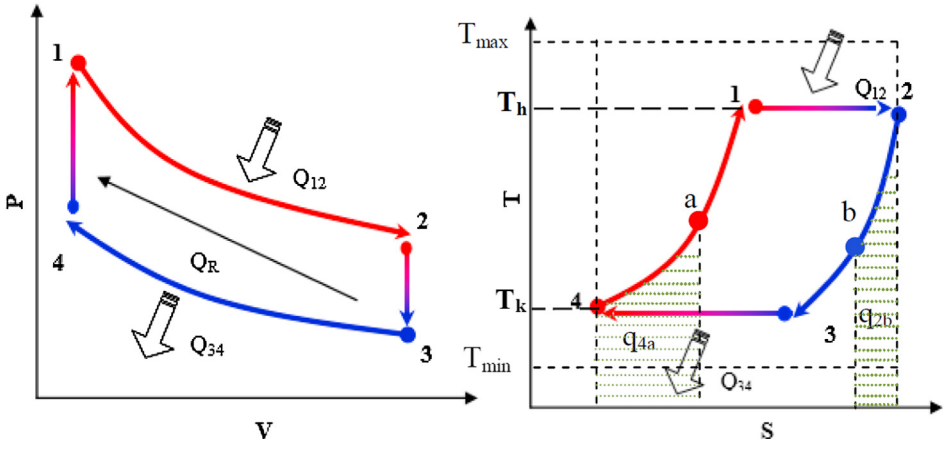

Fig. 2. Theoretical cycle in the P-V and T-S diagrams of a Stirling engine.

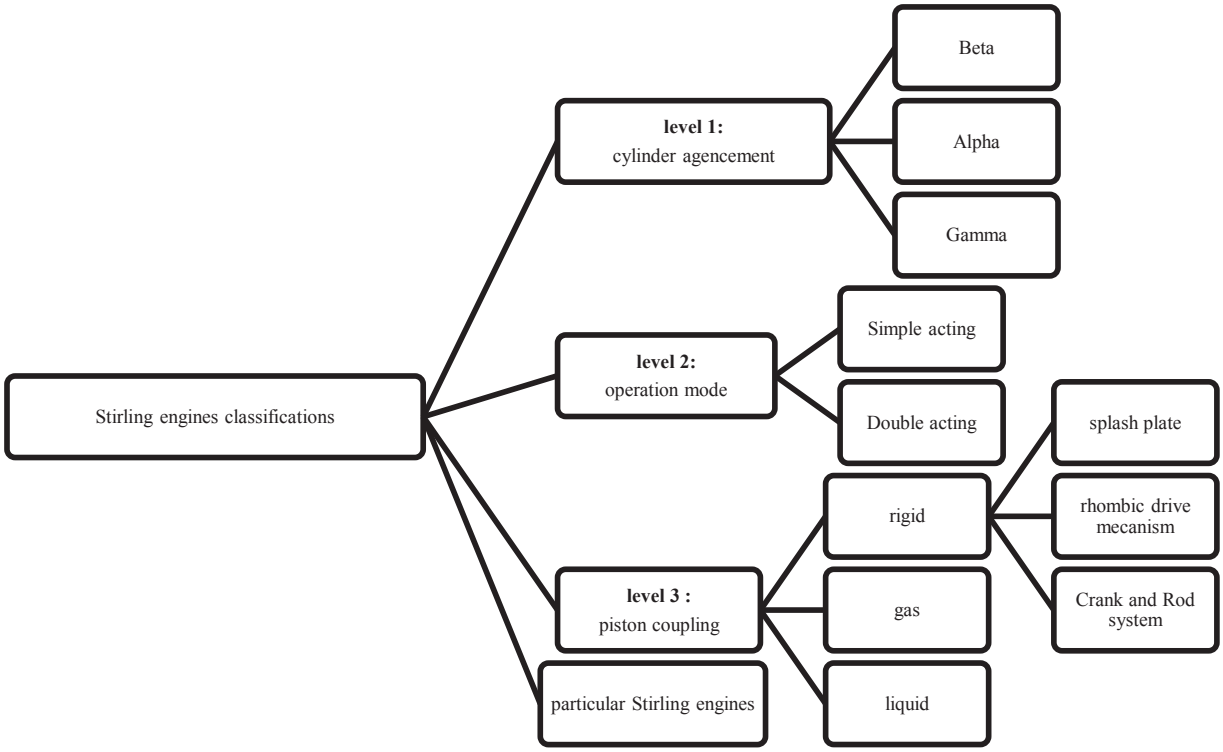

Fig. 3. General classification of Stirling engines.

2.2. Classification

There are three main levels of classification of Stirling machines as it is shown in Fig. 3. According to their operation mode, Stirling machines are devised into two groups (simple acting and double acting machines). Single-acting Stirling engines are constituted by a piston and a displacer, which can be included in the same cylinder or separated into two separate cylinders. However, Double-acting Stirling engines are essentially constituted of two or more pistons [13–15]. Depending on the compression and expansion chambers arrangement; there are three main types of Stirling machines: Alpha, Beta and Gamma (Fig. 4). The Alpha configuration has twin power piston in two cylinders [16–18]. For the Beta configuration, the displacer and the power piston are incorporated in the same cylinder [19–22]. The Gamma configuration uses two separate cylinders, one for the displacer and one for the power piston [23–25]. Recently, Cheng and Yang [26] reviewed the major differences between these three types and investigated its relative performance aiming the optimization of geometrical parameters. According to the pistons coupling, three types of pistons coupling are available in literature: rigid, gas and liquid. Gas coupling machines are known as free piston Stirling machines were invented by Beale [179]. These machines are used in very specific applications, such as in the aerospace industry [27] and it's efficiency is higher than kinematic engines efficiencies because of the absence of driving mechanism (crankshaft, crank rod) [28]. Gas coupling machines are known as fluidyne. Most of the liquid piston Stirling engines were tested for pumping water. It was showed that the practical liquid piston Stirling engines operate at relatively very low temperatures and low frequencies [29]. They are extremely simple and robust and can be easily built with cheap materials in daily life [30]. Wang et al. [30] showed that the fluidyne output power is less than 20 W, and their efficiency is lower than 5%. It is difficult to pressurize the liquid piston Stirling, as the liquid may be spilled out. Rigid coupling pistons are known as cinematic machines. Three different rigid coupling are generally used for Stirling machines: the splash plate, rhombic drive mechanism [19,21,31] and Crank and Rod system [32]. The swash plate mechanism can provide a way of controlling the engine power output by varying the angle of swash plate and thus altering the stroke of the engine [31]. STM 4-120 engine invented in 1958 by Meijer uses the splash plate mechanism. Crank and Rod system is generally used for

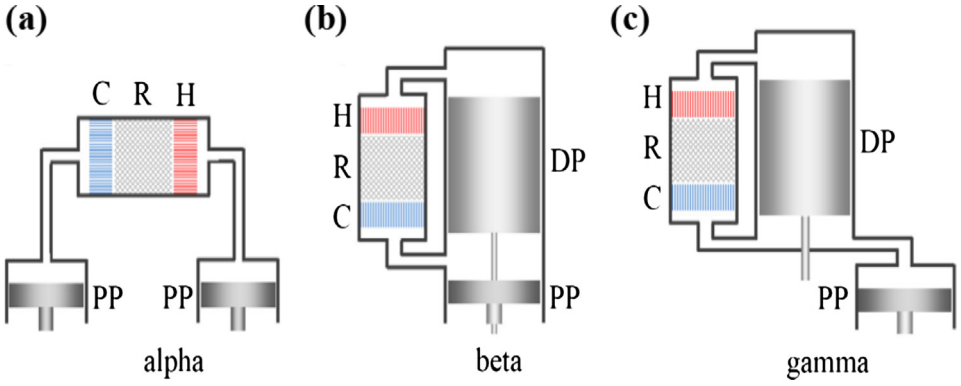

Fig. 4. The three main configurations of Stirling engines: such as C: Cooler, R: Regenerator, H: Heater, PP: Power piston and DP: Displacer [30].

smaller engines [32]. Rhombic drive mechanism has the advantage of being dynamically balanced even for a single cylinder machine [19,21,31]. The comparison with other drive mechanisms shows that rhombic drive mechanism is the most suited drive mechanism for beta-type Stirling engines [200]. In addition to these classifications several particular Stirling engine are available in literature such as thermal-lag Stirling engine (TLE) which is proposed by Tailer [33]. It has only one piston and a porous material stack fixed in the cylinder at the place of the displacer [34]. Other types are the thermo-acoustic machines [38]. Recently, Wang et al. [30] presents a review paper that compare different types of Stirling engines (kinetic, thermoacoustic, free piston and liquid piston). They concluded that kinetic Stirling engines and thermoacoustic engines have the greatest application prospect in low and moderate temperature heat recoveries in terms of output power scale, conversion efficiency, and costs. Their research showed that thermo-acoustic engines for low temperature applications are especially attractive due to their low costs, high efficiencies, superior reliabilities, and simplicities over the other mechanical Stirling engines.

Stirling machines can also be classified as high temperature difference engines or low temperature difference engines depending on the range of temperatures of the hot and cold heat sources, which, in turn, depends on the type of application.

3. Stirling machine applications

3.1. Solar power application

Some industries have developed Stirling engines to use solar energy reflected by a parabolic collector such as contributions infinea [44] or solarDish [45]. Solar dish systems convert the thermal energy of solar radiation to mechanical energy and then to electrical energy similar to the way that conventional power plants convert thermal energy from the combustion of a fossil fuel to electricity [46]. Solar dish systems (Fig. 5) use a mirror array, in the shape of a parabolic dish (1). In order to achieve maximum efficiency, these concentrators are mounted on a structure with two axis tracking system (2), so that the dish can track the sun. The concentrated solar irradiation is absorbed by the receiver and transferred to an engine (3). The engine performances (shaft power, speed, and heating source temperature) increase with increasing solar intensity [47]. An alternator (4) is always coupled to the Stirling engine to convert the mechanical power to electricity. Ref. [46] reported Retired, in operation and under construction solar dish systems.

The most Stirling engines for solar dish systems include the 11 kWe kinematic Stirling engine SOLO 161, the 25 kWe kinematic Stirling engine Kockums 4-95, and the 25 kWe kinematic Stirling engine STM 4-120 [48]. Solar dish systems have demonstrated the highest solar to

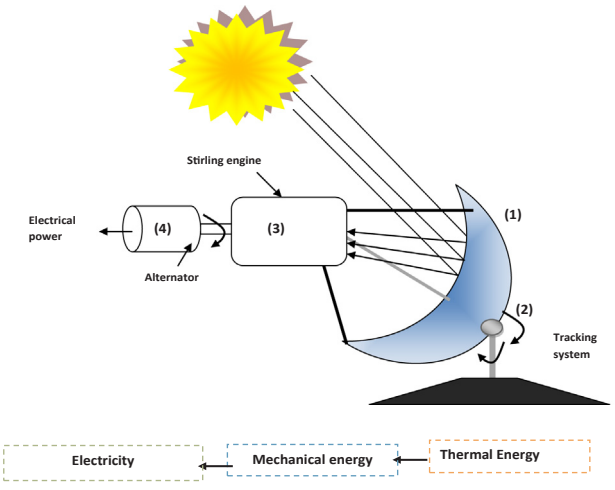

Fig. 5. Solar dish system components and concept.

electric conversion net efficiency. An efficiency of 31.25% achieved by the company Stirling Energy Systems (SES) on February 12, 2008 [49], compared to around 20% of other solar thermal technologies. Yaqi et al. [50], show that the thermal efficiency of SE at optimized condition is about 34%. Solar dish systems are quite heavy weighting about 100 kg/m^2 [51]. These systems have the potential to become the shipper solar thermal technologies. Some researches designed a low cost parabolic solar dish concentrator for direct electricity generation [52]. Table 3 summarizes some available researches using Stirling engines to convert solar thermal energy to electric energy.

3.2. Micro- cogeneration (CHP)

A wide variety of micro-cogeneration systems using Stirling engine coupled to an alternator can be found in literature. Stirling engines are used to produce electricity in micro cogeneration systems typically for domestic use. The six most developed micro-cogeneration units using Stirling engine are listed in Table 4.

Several Stirling micro-cogeneration plants at various stages of development (prototype modeling, dimensioning and fabrication, experimental studies) are described in the literature [63–192]. The role of the Stirling engine in these units is to produce usable electrical energy. One additional advantage offered by Stirling engines is their ability to combust a variety of fuels, such as petroleum and biomass-based fuels. These micro-cogeneration units are classified according to the source of the heat supplied to the Stirling engine summarized in Table 5.

Barbieri et al. [60,61] discussed the feasibility of micro-cogeneration units for residual applications, such as units based on internal combustion engines, gas turbines, Rankine cycle, Stirling engines and generators Thermo-photovoltaic. They showed that the cogeneration system based on the Stirling engine is the best solution in almost all scenarios. Their energy performance has shown that micro-cogeneration units usually satisfy at least 80% of the thermal energy demand, while the ratio of electric power produced to that consumed is usually less than about 85%. De Paepe et al. [62] studied three types of micro-CHP systems for residential use. The different technologies are technically mature, installation costs should at least be reduced by 50% before CHP systems become interesting for residential use. Condensing gas boilers is now very popular in new homes, prove to be economically more interesting and also have a modest effect on primary energy consumption.

3.3. Cryogenic application

Nowadays, Stirling-type refrigeration machines are very well replicated in the field of cryogenics at very low temperatures. They are practically not used in the temperature ranges covered by the steam compression machines, the latter having a better efficiency in this case. These cryo-coolers can liquefy nitrogen (77 K), hydrogen (20 K) or helium (4 K). Several industries have manufactured Stirling cryo-coolers. Industries aim to reduce the size of coolers to the maximum. However, the cooling capacity decreases sharply with the size. This problem is solved when rising pressure and frequency to compensate the volume decrease. Several researchers studied the size limit for Stirling cycle chillers and conducted micrometric chiller investigations.

Domestic refrigeration system using Stirling cycle was first studied by Finkelstein and Polonski [9], Wu et al. [77], evaluated the performance of a Stirling refrigerator (an endoreversible Carnot refrigerator) and calculated the maximum specific cooling load. Chen et al. [78] studied an air refrigeration cycle with non-isentropic compression and expansion. Results show that it exist a maximum value of COP and that the cooling load has a parabolic dependence on COP. He et al. [80] developed a mathematical model based on thermodynamic theory to evaluate the refrigerator lifetime. Results show that the cooling capacity is reduced over 10% at about 631 h and the power consumption of compressor is increased over 20% at about 1168 h. Several numerical

Table 3
Researches from literature using SE to convert solar thermal energy to electric energy.

Reference (Authors)	Engine type	Research Focus
Poullikkas et al. [53]	Kinematic SE	The size of the solar concentrator is determined by the engine capacity. At a maximum direct solar irradiation of 1000 W/m^2, a 25 kWe solar dish Stirling system's concentrator has a diameter of approximately 10 m
Abbas et al. [54]	kinematic SE (Kockums 4–95 SES)	The SE using hydrogen as working fluid in four cylinders of total volume of 380 cc, produces 25 kWe at 1000 W/m^2 with an efficiency between 38 and 40%
Bakos and Antoniades [55]	11 kWe kinematic alpha type SE (SOLO 161)	Carried out a technical feasibility and economic study about large scale Dish/Stirling power plant. The solar plant is made up of 1000 units Dish/Stirling each one produces 10 kWe, while the power conversion unit is the Stirling engine. With this simulation, it is possible to predict annual energy production of 11.19 GWh
Hafez et al. [47]	Different types of SE	Discussed solar dish parameters such as material of the reflector concentrators, the shape of the reflector concentrators and the receiver as well as solar radiation at the concentrator, diameter of the parabolic dish concentrator, sizing the aperture area of concentrator, focal length of the parabolic dish, the focal point diameter, sizing the aperture area of receiver, geometric concentration ratio, and rim angle. Results show that for a 10 kW Stirling engine; the maximum solar dish Stirling engine output power is about 9707 W at 12:00 PM where the maximum beam solar radiation is 990 W/m^2
Barreto et al. [56]	Small scale solar powered β-type SE	Demonstrated that it is possible to obtain an electric power output of 103.8 W with a global efficiency of 10.41% and a thermodynamic efficiency of the SE of 23.75%

Table 4
Characteristics of commercial Stirling engine for micro-cogeneration units (*no longer available).

Micro-cogeneration unit using a Stirling engine	Electric power	Thermal power	Ref.
WhisperGen*	1 kWe	7 kWt	[57]
MEC (Microgen)	1 kWe	3–24 kWt	[59]
Infinia (known under the name of STC)	1 kWe	4–40 kWt	[59]
Disenco (Inspirit)	0.5–3 kWe	12–17.2 kWt	[59]
Cleanergy	2–9 kWe	8–25 kWt	[58]
Qnergy	5 kWe	~24 kWt	[59]

and experimental studies from literature are presented in Table 6.

3.4. Other applications

3.4.1. Automobile propulsion

There have been a few trials to use the Stirling engine as direct propulsion for vehicles [172]. The Stirling engine was placed in a Ford Torino, but the prototype was not developed and the project was abandoned [7]. It was probably related to the engine reactivity for varying mechanical power. The use of Stirling engine for automobile propulsion was a neglected application until it was considered for hybrid cars. Hachem et al. [173] investigates an exergetic analysis of a heat recovery system using double acting type Stirling engine to recover the exhaust heat of internal combustion engine. Alfarawi et al. [68] predict the thermodynamic performances of a recovery system using Beta type Stirling engine to provide electricity for car's electronic devices instead of taking power directly from the internal combustion engines drive shaft. Their results show that it is possible to generate a power output of 1.5–2 kWe at an ideal thermal efficiency of 40% and engine overall weight of 11–14 kg. Huang et al. [75] investigates experimentally a recovery system coupling exhaust gas from gasoline engine to a Beta type SE with rhombic-drive mechanism. Results showed that it is able to recover only 247 W electric power and 1.3 kW indicated power at 14 bar and 840 rpm.

3.4.2. Space application

Some satellites get electrical power through Stirling engines. Their efficiency is particularly high due to the great differences of temperature in the space. The hot source consists of radioactive isotopes [86]. The nuclear fission heat generated in the reactor core with the temperature of about 1200 K is considered as the hot source. Part of the heat is absorbed by the hot heat exchanger and converted into electrical power and the exhaust heat is rejected from the cold side [86].

4. Technological challenges

4.1. Control problem

Knowing that, any thermal engine is exposed to continuous internal and external perturbation while operating. And that the SE mechanical

Table 5
Numerical studies from the literature: Stirling engine power and working conditions.

Investigator(s)	Year	Micro-cogeneration unit	Stirling output Power	Working conditions				
				Working gas	Pressure (bar)	Speed (rpm)	Source of the hot source	Hot temperature (°C)
Podesser et al. [73]	1999	–	3.2 kW	N_2	33	600	Biomass combustion	–
Obernberger et al. [4]	2003	–	35 kW	H_e	45	1000	Biomass combustion	300
Thiers et al. [74]	2010	Sunmachine Pellet micro-CHP unit.	1.5–3 kW	N_2	33–36	500–1000	Biomass combustion	600–800
Parente et al. [65]	2012	SOLO Stirling 161 Cogeneration Unit	2 to 9 kW	H_e	40–150	–	Natural gas combustion	550
Cacabelos et al. [67] Valenti et al. [69–70]	2015	Whispergen unit	1 kW	N_2	20–28	1500	Natural gas combustion	700
Sowale et al. [187]	2018	Stirling engine integrated with a self-sustaining sanitation technology	0.27 Wh	air	10	1431	Biomass combustion	500
Çinar et al. [199]	2018	Alpha-type Stirling prototype	30.7 W	H_e	3.5	437	Electrical heater	1000

Table 6
Stirling cooler performances and working conditions.

Investigator(s)	Type	Stirling cooler performances		Working conditions				Experimental study	Numerical study
		Cooling capacity (W)	COP	Cold end temperature (K)	Charged pressure (bar)	angular speed (rpm)	Working fluid		
Ataer et al. [81]	V-type Stirling refrigerator	33–83	0.6–2.2	240–270	2	1000	air		X
Le'an et al. [10].	V-type Stirling cooler (VISR)	5–80	0.1–0.9	238	2.5–14	200–1000	He or N_2	X	X
Zhu et al. [82]	Pulse tube type Stirling refrigerator	200–1800	0–0.2	77	25	3000	He		X
Chin-Hsiang CHENG et al. [21]	Beta type Stirling cooler with rhombic drive mechanism	3–8	0–0.4	90–200	1–3	1000	He	X	X
Tan et al. [83]	Pulse tube type Stirling cryocooler (PTR)	4–10	0.08–0.21	80	33	2640	He		X
Caughley et al. [84]	Free-piston Stirling cryocooler	29	0.17–0.29	77	1–5	300–3000	He		X
Wang et al. [85]	Two-stage high-capacity free-piston Stirling cryocooler	65	0.22	30	30	2400	He	X	X

output power must be provided at a rotation speed adapted to the receiver system operation (usually a generator in Solar and micro-CHP applications). Thus, in order to regulate the Stirling engine performances under the conditions of its use, it is important to forecast a mechanical output power control system. Previous researches show that the Stirling engine cannot change speed quickly [87]. And there are four methods in the literature to control the mechanical power of such engine [88]:

(a) Mean pressure control

The power developed by a SE can be controlled by regulating the pressure throw an external compressor. The simplest method of reducing the engine power is to remove an amount working gas from the engine and supplying gas by an external compressor when more power is needed [89,90]. The Kockums/SES 4-95 and SOLO 161 engines use this control method [91]. However, this method requires careful monitoring of the time intervals and the degree of valves opening when using the external compressor [90]. The 225 kW double acting Stir1ing engine developed by MAN Technology uses Helium as working gas under high mean pressure. Since engine output is influenced by the working gas pressure, the SE mechanical output power is regulated by changing its mean pressure [3]. Hachem et al. [87] showed that, when using the mean pressure control method, irreversibilities inside the engine increases. They showed that the pressure increase enhances the Stirling cycle power and efficiency until an optimum value. Thus the mean pressure control method increases irreversibilities inside the engine.

(b) Piston stroke control

Fast power control is now possible using pistons strokes control system, making it possible to change the power levels in a fraction of a second. With a compact drive design and modern materials, the specific power can be the same as that of the modern gasoline engine [172]. When increasing the piston stroke, the output power decreases. This technique can be applied to single or double acting engines and even to free-piston engines. The swash plate mechanism with variable shift angle is used by the STM 4-120 to control the mechanical engine power [92]. The successful introduction of the swash plate mechanism has ameliorated the situation of the Stirling engines compared to internal combustion engines. Now the multiple-valve gasoline engine looks sophisticated compared to the four-cylinder variable swash plate engine [172].

(c) Shift phase control

This control method is one of the best ways to quickly control the SE mechanical output power. However, this method cannot be applied to Stirling double-acting engines [174]. A motion conversion system was introduced by Marks [93] in order to amend the stroke and the shift phase of the pistons. The proposed mechanical system is a good solution to provide rapid engine power control.

(d) Dead volume control

The SE mechanical output power decreases with its internal dead volume increase. Although dead space represents an un-useful volume that needs to be reduced, a power control method involves varying the dead volume by opening a valve to incorporate additional volume into the engine's thermal circuit. As the dead volume is reduced the mass flow increases [88]. In fact, when an additional dead volume is added to the engine circuit, this extra space is filled with mass, thus the mass flow at the engine exchangers decreases. In particular, Philips laboratories prefer this control system rather than the pressure variation control system [7]. Recently, Beltran-Chacon et al. [88] proposed a

system with an extra dead volume of 160–0 cm^3 to control the SE mechanical output power. Their results show that the effect produced by reducing the extra dead volume is very similar to the effect produced by the increased mass of the working fluid (using the mean pressure control method). When the mass flow decreases, the hot end temperature increases. At low radiation, a mass flow rate of 81 g/s achieves the highest engine power with a corresponding extra dead volume of 160 cm^3.

4.2. Sealing and leakage of gas

In Stirling engines, the working gas leaks are a major difficulty since the engine operates under high pressure, until 200 bar [94]. Losses due to gas leakage reduce considerably Stirling engine performances. Kato et al. [96] show that the gap between the displacer and displacer chamber wall should be reduced to obtain a high average temperature in the hot chamber. Recently, Sauer et al. [95] presents a numerical simulation that directly takes into consideration the interactions between the cylinder wall temperatures and the overall gap loss. Results underline the advantages of comprehensive models and the need to apply them for advanced design optimization purposes.

4.3. Thermal and mechanical losses

The operation process of the Stirling engine is based on the cyclic compression and expansion of a set quantity of working fluid. Due to the heat exchange between the working gas and essential elements (regenerator, heater and cooler) a temperature difference appears along the engine which is the seat of many thermal losses [97]. A simplified mapping of this kind of engine is presented in Fig. 6. Thermal and mechanical losses are reported in the maps.

Several thermodynamic modeling that takes into account thermal and mechanical losses inside the Stirling engine are presented in Table 7. Cun-quan et al. [98] established a theoretical model to predict the dynamic performance of a new type of pneumatically-driven split-Stirling-cycle cryocooler. The model takes into account the compressor working characteristics and the significant losses of cooling, including regenerator inefficiency loss, solid conduction loss, shuttle loss, pump loss and radiation loss. Results show that the gas pressure has amplitude attenuation and phase delay effects and the gas mass flow rate remain the same from the compressor to cold chamber. Tlili et al. [99] estimated the pressure drop in a GPU-3 heat exchangers. The energy lost average due to pressure drop is 934.9 W in the regenerator, 123 W in the heater and 26.57 W in the cooler. They proposed to improve the heater convective heat transfer coefficient by investigating different surface shapes.

4.4. Lubrication challenge

According to Makhkamov and Ingham [182], the mechanical loss for some particular designs of the Stirling engine may be up to 50% of the indicated power of the engine; it could from friction between two moving parts, vibration, poor mechanism design, interference among parts, thermal deformation or lubricant degeneration, etc. Typically, mechanical loss increases with rotation speed of the engine. One of the disadvantages of Stirling engines having a mechanical training system is the energy loss due to friction. To minimize this loss, the lubrication becomes necessary. However, in Stirling engines, the lubrication generates negative effects by creating a lubricant layer over heat transfer surfaces of heater, regenerator and cooler. That is why, the training system should be designed so as to work with a little lubrication or totally dry. Altin et al. [181] assumed that alpha type Stirling engines with Scotch Yoke piston driving mechanism are expected to have relatively lower lubrication requirement. As the result of low lubrication, the heat exchange performance of the working fluid should be increased. Due to the increase of the inner heat transfer performance of the engine, a higher thermal efficiency and power density may be expected.

4.5. Production cost problem

The SE was invented over 200 years ago, it has significantly higher production cost than other heat engines [109]. Because of the high pressure (> 200 bar) and high temperature (> 700 °C), Stirling Engines are expensive to build. Moreover, the choice of the “ideal” gas can bring some difficulties associated with its ability to diffuse through materials [175]. Low cost Stirling engines exist, but they are small and only suitable for small powers. Stirling engines prices are different and depend on the engine’s maximum electric output power and efficiency. Only few companies sell SE installation. However, with new research, it is possible to overcome the engine technical challenges, which will increase the demand for the SE [110]. Based on a cost analysis, Gadré [109] concluded that the major cost components in the SE are the hot heat exchanger and the regenerator. The hot heat exchanger as well as the regenerator requires material that can obtain a high temperature difference under high pressure, and the materials that can do so are very expensive. Few researches focus on reducing the material cost of heat exchangers such as Abduljalil et al. [111] how identified a low-cost material of the regenerator with performance similar to those usually used materials. The major researches available in literature focus on technical improvements to increase the SE efficiency and mechanical output power. Ferreira et al. [110] identified every component cost of a solar-powered Stirling engine plant able to produce 3.65 kW of electrical power and 11.1 kW of thermal power (Fig. 7). Their results show that the two most expensive components are the Stirling engine and the

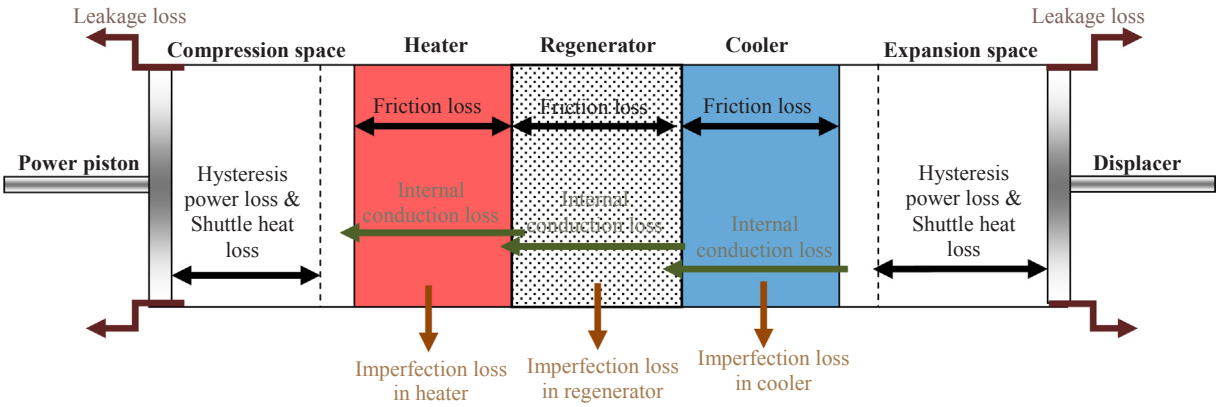

Fig. 6. Diagram representing the location of various energy losses in a Stirling engine.

Table 7
Available models from literature.

Auteur	Stirling engine type	Model	Losses							
			Friction loss	Regenerator imperfection loss	Internal conduction loss	Heater and cooler imperfection loss	Shuttle heat loss	Hysteresis power loss	Leakage loss	Mechanical pressure drop
Araoz et al. [101]	All types of engines	Second order model	X	X	X					
Paul et al. [102]	Stirling GPU-3	Second order adiabatic model	X	X			X	X		
Campos et al. [103]	A double-acting Stirling engine having an oscillating plate drive mechanism	A model, which combines empirical correlations, and thermodynamics								
Parlak et al. [25]	Gamma type Stirling engine	Non-ideal Adiabatic model					X	X	X	
Li et al. [24]	Gamma type Stirling engine	First order isothermal model combined with thermodynamics in finite time.	X	X	X					
Babaelahi et Sayyaadi [104–106]	Stirling GPU-3	Stirling engine polytropic analysis With various losses (PSVL)	X				X		X	
Hosseinzade and Sayyaadi [107]	Stirling GPU-3	Adiabatic model combined with finite time thermodynamics: CAFS (Combined Adiabatic-Finite Speed)	X	X						
Hachem et al. [97]	500 W Gamma type Stirling engine	Quasi-steady model with losses	X	X	X	X	X			X
Bataineh [183]	alpha –type mean differential Stirling engines utilizing Ross Yoke drive mechanism	Second order numerical model considering losses	X	X	X					
Xiao et al. [184]	100 W ß-type Stirling engine	An Improved Simple Analytical Model (a third-order model, Sage, improved by a second-order model)						X	X	X

heater. Their costs represent respectively 24% and 30% from the total cost of the system.

5. Modeling and optimization

5.1. Modeling

A key issue in designing and optimizing Stirling engines is to build a precise model to predict output power, thermal efficiency and provide useful information for further improvement. Different models are established in order to optimize Stirling performances. Such as Finite Time Thermodynamic analysis, Finite speed thermodynamic analysis, Isothermal model, Non-ideal adiabatic method, CAFS: The Combined Adiabatic- Finite Speed Thermal Model and Polytropic analysis of Stirling engine with Various Loss mechanisms (PSVL) model. Ahmadi et al. [42] compared the conventional thermodynamic methods for GPU3 Stirling engine. The outcome of his comparison revealed that PSVL was better than the other methods. Five types of analysis are available in literature: zero order modeling, first order modeling, second order modeling, third order modeling and CFD simulations.

5.1.1. Zero order modeling

The zero order analysis is based on experimentation. It consists of directly expressing power supplied by the engine or the cooling capacity of the Stirling refrigerator [29]. This method was carried out by Williams Beale [179]. He proposed a semi-empirical expression to calculate the power of a Stirling machine operating as an engine as follows:

$$W_m = K \bullet P \bullet f \bullet V_{sc} \tag{8}$$

where K is the power correction factor, V_{sc} is the swept volume of the compression space (m^3), f is frequency (Hz) and P is the mean pressure (Pa). This equation was confirmed by West [178] and Organ [180]. West [178] proposed a second expression to express the mean power of a SE:

$$W_m = 0.25 \bullet P \bullet f \bullet V_{sc} \tag{9}$$

5.1.2. First order modeling

The first analysis of the Stirling engine is isothermal analysis. It was published by Professor Gustav Schmidt [39]. This analysis is considered the simplest. And it adopts several simplifying hypotheses: the compression and the expansion are made in an isothermal way, the regeneration is perfect and the pressure throughout the engine is supposed to be uniform. Adiabatic analysis was made by Finkelstin [40]. He assumed that heat transfer in work spaces occurs by convection. Since the variation in gas temperatures leads to temperature discontinuities. Finkelstein introduced the concept of conditional temperatures as a function of the direction of the flow of the working gas. The compression and expansion are considered adiabatic. The working fluid behaves like a perfect gas. The pressure is uniform in the engine. The regenerator is perfect and has a linear temperature distribution. No leakage of working fluid is noted. All processes are reversible. Adiabatic and isothermal analysis are said to be of the first order analysis. Adiabatic analysis was reconsidered by Lee [41] and by Urieli and Berchowitz [7]. Urieli and Berchowitz [7] also analyzed different engines using the ideal adiabatic model. They agree that the isothermal and adiabatic models do not take into account losses within the Stirling machine. In actual engines, the obtained theoretical efficiency differs from the experimental values. These engines have many losses, such as gas leakage losses, friction losses, heat losses, losses due to piston movements and other [43].

5.1.3. Second order modeling

Second order analyzes consist of correcting first order analyzes to consider thermal losses and friction losses within a Stirling engine. In

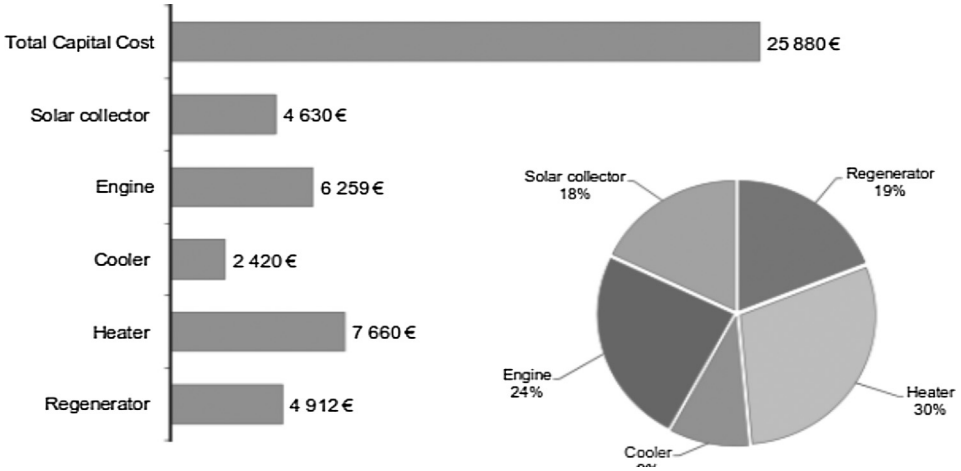

Fig. 7. Total capital cost and relative capital costs for each component for a solar-powered Stirling engine plant able to produce 3.65 kW of electrical power and 11.1 kW of thermal power. (reprinted from Ferreira et al. [110] copyright 2016 from Elsevier).

second order analysis, the different losses are independent and are calculated separately. They can be classified into two categories: power losses and thermal losses [2]. According to ref [97], losses can be classified into losses due to piston movement, losses in heat exchangers and friction mechanical losses. The most significant losses for the Stirling engine are depicted in Table 8. Using a second order numerical model that considered thermal, pumping and regeneration losses. Bataineh et al. [183] showed that engine performance improvements can be achieved by : decreasing thermal conductivity of regenerator matrix, increasing regenerator heat capacity, optimizing regenerator volume, optimizing working frequency, and optimizing working gas mass.

5.1.4. Third order modeling

Third order modeling is based on the resolution of Navier Stokes and energy conservation equations to determine instantaneous evolutions of velocity, pressure and temperature of the working fluid at each working space (compression and expansion chambers and the tree heat exchangers). The resolution of the extended Brinkman-Lapwood-Forchheimer Darcy model is used to determine heat transfer and flow in the porous medium (regenerator). These analyzes describes more precisely thermo and hydrodynamic processes that take place in the Stirling engines. Xiao et al. [184] tried to improve a third-order model, Sage, by a second-order model. And suggested an improved simple analytical model that considered effects of seal leakage loss, gas spring hysteresis loss and piston friction loss.

5.1.5. Computational fluid dynamics simulation CFD

CFD approach allows the heat transfer characteristics to be investigated in great detail. Results describe the behaviors of temperature, pressure and velocity in different spaces and especially in the regenerator [185]. Evidently, second order thermodynamic analysis is simpler and less time consuming than CFD. However CFD considers more details as well as the engine geometry and consequently reflects more details about the flow field and losses phenomena. Mohammadi et al. [186] evaluated the influence of turbulence modeling. Simulations were repeated employing k-ω SST turbulence model. Their results showed less than 1% of change in engine power while assuming turbulent flow.

5.2. Optimization

5.2.1. Optimization criteria

Optimization criteria are also called objective functions are devised into technical criterions and economic criterions.

5.2.1.1. Technical criterion.

(a) Energy efficiency

Energy efficiency is the most understandable and considered criterion by industry because it reflects a real and direct economy of the consumed energy. Energy efficiency is a purely quantitative criterion and does not take into account the quality of the energy consumed, produced and rejected.

The SE thermal efficiency η_{th} is defined by:

$$\eta_{\mathrm{th}} = \frac{\text{Produced work}}{\text{amount of heat received by the working fluid}} = \frac{-\delta W}{\delta Q} \tag{10}$$

The Stirling refrigerator coefficient of performance is defined as the ratio of the desired output effect (cold calories) to the power consumed by it as follow:

$$\mathrm{COP_R} = \frac{\text{desired output}}{\text{required input}} = \frac{|Q_L|}{W_{in}} = \frac{|Q_L|}{Q_H - Q_L} = \frac{1}{(Q_H/Q_L) - 1} \tag{11}$$

where T_H is the high source temperature and T_L is the cold source temperature. Q_H and Q_L are respectively amounts of heat rejected to the high source and received from the cold source during one cycle.

The Stirling heat pump coefficient of performance is defined as the ratio of the desired output effect (hot calories) to the power consumed by the heat pump:

$$\mathrm{COP_{HP}} = \frac{Q_H}{W_{in}} = \frac{Q_H}{Q_H - Q_L} = \frac{1}{1 - (Q_L/Q_H)} \tag{12}$$

(b) Exergy efficiency

Exergy efficiency is used by scientists to perform the quality of energy. It is defined as the ratio of the actual thermal efficiency to the maximum possible (reversible) thermal efficiency under the same conditions. The system exergy efficiency can be expressed as the ratio of the exergy recovered (as useful input) and the exergy supplied (as total input). For a heat engine, the exergy efficiency is expressed as follow:

$$\eta_{\mathrm{Ex}} = \frac{W_{out}}{\left(1 - \frac{T_0}{T_H}\right) Q_H} \tag{13}$$

where W_{out} is the actual output work, Q_H is the amount of heat received by the working gas, T_H is the mean hot end temperature and and T_0 is the reference temperature which is taken as the ambient temperature.

For a Stirling refrigerator, heat is transferred from a high temperature medium to a lower temperature medium. The exergetic

Table 8
Description of different losses inside the SE from literature.

Losses		Description	Ref(s)
Losses due to pistons movement	Shuttle heat loss	This loss is due to the Shuttle movement of the piston between the top dead center (TDC) and the bottom dead center (BDC) of the cylinder. The latter has a temperature of the expansion space higher than the temperature of the compression space. Therefore, the piston transports heat from the hot side to the cold side return	[97]
	Hysteresis power loss	This loss is due to the existence of a clearance between the piston and the wall of the cylinder creates a cyclic flow of the fluid from the expansion space to the compression space or vice versa. Since the temperature levels are different in the two cylinder spaces, additional heat loss is caused by this flow	[24]
Heat exchangers losses	Imperfect heat loss	Heater, cooler and regenerator like any heat exchangers are not perfect. The average air temperatures respectively inside heater, cooler and regenerator are lower than their wall temperatures	[99]
	Internal conduction loss	This loss is due to the important gradient of temperature exist between Stirling engine interfaces leading to an internal conduction loss through regenerator, heater and cooler. This loss is calculated with in the two sections of the heat exchangers	[97]
	Viscous friction power loss	This loss result from the viscous friction of the working gas as it passes through the singularities of the Stirling engine, essentially the heat exchangers and the regenerator	[97]
Mechanical friction power loss		This loss result from friction losses of moving mechanical parts. It depends on the drive system	[97,100]

coefficient of performance of the refrigerating machine COP_{ExR} is expressed as follows:

$$COP_{ExR} = \frac{\left(1-\frac{T_0}{T_L}\right)|Q_L|}{W_{in}} \quad (14)$$

where T_L is the cold end temperature, Q_L is the amount of heat received from the low-temperature reservoir (the desired effect from the refrigerator) and W_{in} is the actual work input (the power consumed by the refrigerator).

For a Stirling Heat pump, heat is transferred from a low temperature medium to a higher temperature medium. The exergetic coefficient of performance of the heat pump COP_{ExHP} can be calculated as follow:

$$COP_{ExHP} = \frac{\left(1-\frac{T_0}{T_H}\right)Q_H}{W_{in}} \quad (15)$$

where T_H is the hot end temperature and T_0 is the reference temperature. Q_H is the heat supplied to the hot reservoir (the desired effect from the heat pump) and W_{in} is the actual work input (the power consumed by the heat pump).

5.2.1.2. Economic criterion. There are several criteria for assessing the economic profitability of the facility such as the Levelized Cost of Electricity (LCOE) [112,113], Life Cycle Cost Savings (LCCs) and the period of return on investment (Pay Back time, PBT). The life-cycle cost saving (LCCs) is defined as the difference between the cost of the installation over its entire life cycle and the cost of a traditional installation using only fossil energy [114]. This corresponds to the cost which would be saved thanks to the use of micro-CHP systems or solar Dish installations. The PBT is the length of time the project takes to retrieve the initial investment [115]. These criterions are usually used in assessing the economic feasibility micro-CHP or solar dish systems using Stirling engine technology. Several researches investigate the cost of such systems. Arora et al. [137] define a Thermo-economic function that includes annual investment cost, energy consumption cost and maintenance cost in order to analyze a dish collector with parabolic arrangement of mirrors collecting solar energy on a focal point that acts as high grade input heat energy for Stirling engine. Results show that the power output, the overall thermal efficiency and the thermo-economic function are respectively 38.96 kW, 23.92% and 0.3124 which are 17.09%, 35.09% and 10.74%, respectively lower in comparison with reversible system. Ferreira et al. [110] introduced a costing methodology of a solar powered Stirling engine for micro cogeneration. Such as each system component is represented by a cost equation. The thermo-economic model predicts the best economic output for the best combination of geometrical and operational parameters of the system on a cost-effective way. Results show that the best configuration depicts a cogeneration system able to deliver 3.65 kW of electrical power and 11.06 kW of thermal power for a residential building and saves 627 €/year. Ust at al. [176] introduced a new ecological objective-function that always has positive values to identify the effect of loss rate of availability on the power output. The objective function is called the ecological coefficient of performance (ECOP) and defined as the power output per unit loss rate of availability.

5.2.2. Making decision methods

The search for optimal parameters of Stirling engines can be done in different ways using uni-variant methods or multi-objective method. Major researchers uses results from mathematical modeling in Stirling engine optimization. Others use directly their experimental results for the optimization. Various multi-objective making decision methods are employed to maximize output power and efficiency, to minimize losses and cost. Such as experimental design methodology [116], particle swarm optimization method (PSO), artificial neutral network methods (ANN) and genetic algorithm methods (GA).

5.2.2.1. Uni-variant method. The uni-variant method is the classic study [117–120]. This method allows studying only the influence of a single parameter. All other parameters are set to well-known values, and only the parameter to be studied varies. In this approach, we can study any parameters (independent or not).

5.2.2.2. Multi-objective methods.

(a) Experimental design methodology

The experimental design methodology was developed by Fisher [121]. It allows a better organizing experimental trial in scientific research [122]. It reduces the number of tests to be carried out to scan the entire field of study, gives the possibility to study a large number of factors at once and can detect single or double interactions between the factors studied. In Ref. [116], Gheith et al. uses the experimental design methodology to study the effect of four operation parameters on the asymmetry of temperature between both regenerators' sides. The heating temperature, the charge pressure, the cooling water flow rate and the operation time were chosen as independent factors. Their results show that the charge pressure and the heating temperature have the largest effect on Stirling engine brake power, whereas, the cooling water flow rate marginally influences the engine brake power. Only the interaction between the charge pressure and heating temperature and charge pressure and cooling water flow rate are significantly affecting the Stirling engine brake power. Results show that optimal conditions for the functioning of Gamma type SE are 355 W of brake power for a

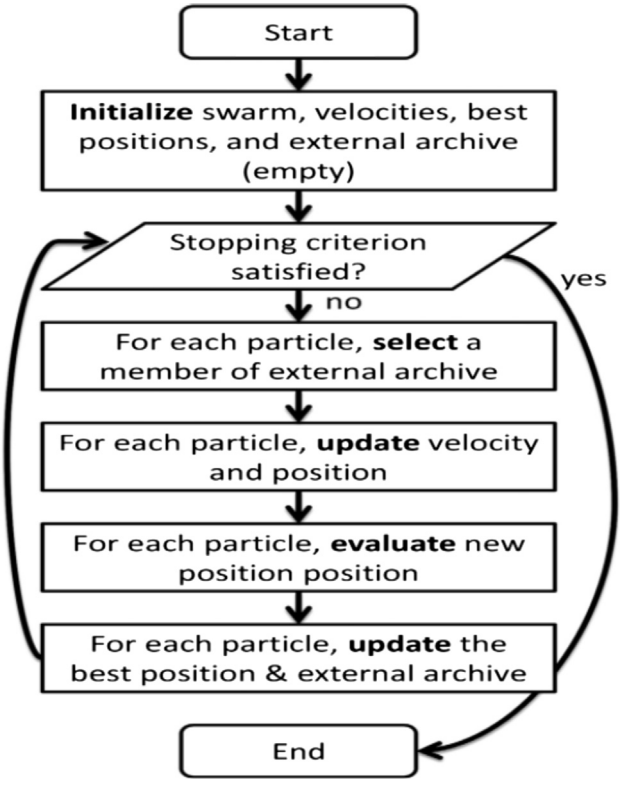

Fig. 8. Working principal of PSO (reprinted from Duan et al. [124] copyright from Elsevier).

charging pressure of 8 bar, a heating temperature of 500 °C, and a cooling water flows of 7.3 l/mn.

(b) Particle swarm optimization (PSO) method

Particle Swarm Optimization method (PSO) was first proposed by Kennedy and Eberhart [123]. PSO method is a computational method that optimizes a problem by iteratively trying to improve a candidate solution with regard to a given measure of quality. PSO method is used for the multi-objective optimization [124]. This method was applied in the area of designing Stirling engine in Ref. [124]. PSO is highly competitive and can be considered a viable alternative to solve multi-objective optimization problems. In addition, the exceptionally low computational times required by PSO approach make it a very promising approach to problems (e.g., engineering optimization) in which the computational cost is a vital issue [123]. Fig. 8 describes the working principle of each method.

(c) Artificial neural networks (ANNs)

Artificial neural networks (ANN) is a logic programming technique developed with the purpose of automatically performing skills such as learning, remembering, deciding and inference, all features of the human brain, without receiving any aid. ANNs while implemented on computers are not programmed to perform specific tasks. Instead, they are trained with respect to data sets until they learn the patterns presented to them. Once they are trained, new patterns may be presented to them for prediction or classification. Özgören et al. [125] applied artificial neural network (ANN) to predict the torque and power of a beta-type Stirling engine using helium as the working fluid. Tavakolpour-Saleh et al. [126] used an ANN controller with an optimal configuration is thus proposed to control the engine frequency based on the observations of water head, sink temperature and collector temperature. ANNs working principle is described in Fig. 9.

(d) Genetic algorithm (GA)

Some researchers had applied GA to optimize Stirling engine performances. Genetic algorithms are known as the most effective evolutionary algorithms inspired by both natural selection and natural genetics that can be effectively applied to complex optimization problems. Its working principle is presented in Fig. 10. The effective working of GA and PSO requires determination of control parameters in addition to common parameters like population size and number of generations [128]. However, there are two main differences between PSO and GA [130]. Firstly, genetic algorithms rely on three mechanisms in their processing: parent representation, selection of individuals and the fine tuning of their parameters. On the contrary, PSO only relies on two mechanisms because it does not adopt an explicit selection operator. However, the absence of a selection mechanism in PSO is compensated by the use of leaders to guide the search. A second distinction has to do with the way in which the individuals are manipulated. PSO uses an operator that sets the velocity of a particle to a particular direction. This can be seen as a directional mutation operator in which the direction is defined by both the particle's personal best and the global best of the swarm. If the direction of the personal best is similar to the direction of the global best, the angle of potential directions will be small, whereas a larger angle will provide a larger range of exploration. In contrast, GA uses a mutation operator that can set an individual in any direction, although the relative probabilities for each direction may be different (see Fig. 11).

Two types of GA are available according to the use. The difference between these algorithms is described below:

(d.1) Single-objective evolutionary algorithm (SOEA)

This type of algorithm is used when developing an optimization according to a single criterion. For example: the NOMAD algorithm. The "NOMAD" algorithm belongs to the family of direct search algorithms (Mesh Adaptive Direct Search algorithm, MADS) which is itself an extension of the generalized pattern search method Search algorithm, GPS). This type of algorithms is well suited for optimization functions whose calculation is generated by an extensive calculation and which have one or more of the following properties [129]:

- has no exploitable properties such as derivatives
- may be contaminated by digital noise
- may fail to give results even for points that belong to the feasibility area

(d.2) Multi-objective evolutionary algorithm (MOEA)

Although many researchers have worked on the development and optimization of Stirling engine, but most of them have focused on single objective solution. Multi-objective optimization gives uncountable set of solutions called as Pareto Front. Recently, Multi objective techniques have been applied with different Stirling engine models by some authors [109–118]. Theses researches are presented in Table 9.

5.2.3. Optimizations parameters

In order to optimize Stirling engine, four types of parameters can be investigated.

5.2.3.1. Geometric parameters.

(a) Compression ratio

In a Stirling engine, the compression ratio is defined as the ration between compression volume V_{com} and expansion volume V_{det}. The compression ratio is actually determined by the combination of geometrical parameters such as the strokes of displacer and power piston, the radius of displacer and power piston, and length of displacer. The

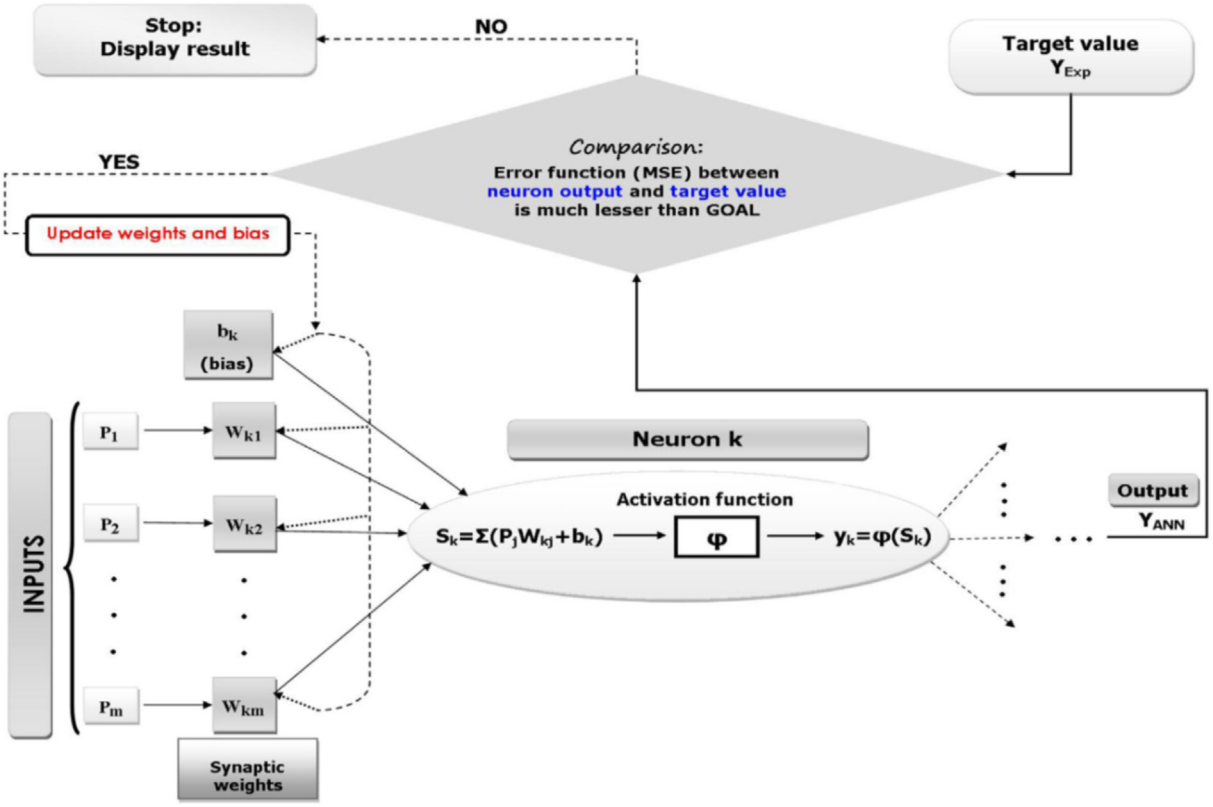

Fig. 9. Working principal of ANN (reprinted from Ahmadi et al. [127] copyright 2015 from Elsevier).

magnitudes of the impact produced by the individual parameters on engine performance could be different; hence engines designed with the same compression ratio but through different combinations of these parameters could perform differently [138]. Walker [1] has shown that SE power depends on the compression ratio. The optimal compression ratio τ varies with the temperature rate. Recently, Erbay et al. [139] investigated thermodynamically the duplex type Stirling refrigerator by considering the combined effects of diverse constructional and operational parameters which are namely temperature ratios and compression ratios. Results show that the work rate increases when the swept volume in the cylinder becomes big or when the temperature difference between the heat source and sink rises. Erbay et al. [139] investigated thermodynamically the duplex Stirling by considering the combined effects of diverse constructional and operational parameters which are namely the temperature ratios for heat engine and refrigerator and the compression ratios for both sides. Results show that the heat engine cannot meet the demand of the cooler at the higher temperature ratios when the compression ratio is beyond 10. Chen et al. [138] investigates geometrical parameters in a low temperature differential Gamma type SE. They found that power piston stroke and radius influence engine performance very similarly, and that power and efficiency both increase as these two parameters increase. If the power piston stroke is limited, the same compression ratio can be achieved by adjusting the radius of power piston, and vice versa. A larger compression ratio creates larger pressure variations in both working spaces [138]. Thus, Stirling engine mechanical output power and efficiency increase with compression ratio.

(b) Phase angle between the power piston and the displacer piston

Phase shift of about 90° between the power piston and the displacer piston is generally applied. This is typically accomplished with mechanical linkages that connect the crank shaft to the displacer. Depending on the engine actual design and on the gas flow path, the

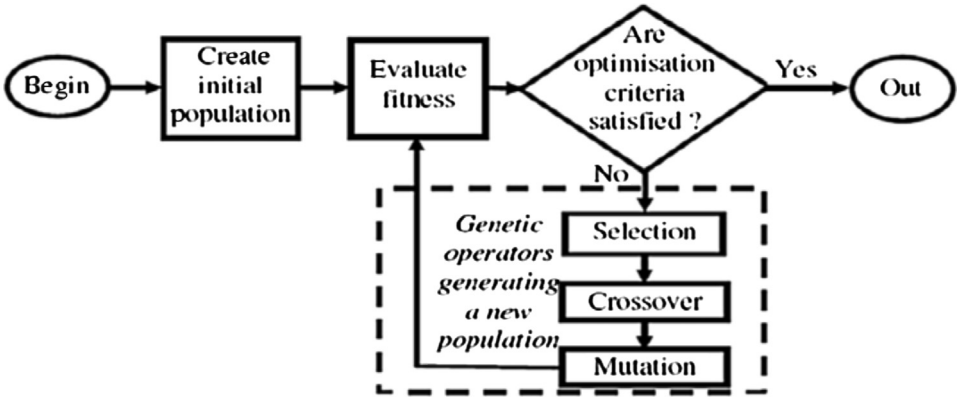

Fig. 10. Working principal of GA (reprinted from Zare et al [128] copyright 2016 from Elsevier).

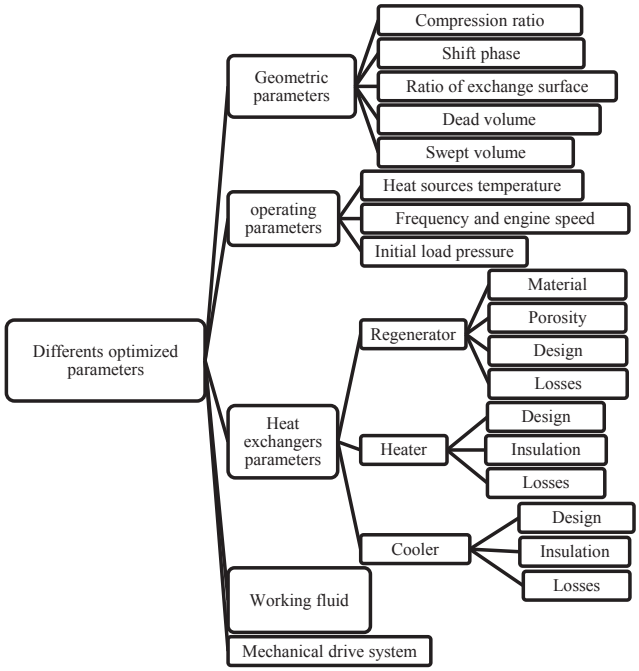

Fig. 11. Different types of optimized parameters.

ideal phase difference may be less or more than 90°. The working piston and the displacer are connected by a motion converting mechanism; the phase angle between pistons is not arbitrary [1]. According to Walker [1], when the temperature rateT_{com}/T_{det} is between 0.35 and 0.5; the dimensionless power is maximum for a phase angle between 90° and 115°[1]. Chen et al. [135] approved that the ideal working domain for displacement phase shift is neighborhood interval of 90°. When optimizing a free displacer (FPFD) Stirling cryocooler performances. As far as, Zhu et al. [82] endorsed that the optimum phase angle for cooling power is larger than that for the COP for the pulse tube Stirling refrigerator. Alfarawi et al. [140] show that power increases as phase angle increases up to an optimum value then it falls down. The optimum value exists as a result of balance between increased gas volumetric exchange and compression ratio, and the elevated pressure drop in the regenerator. The maximum indicated power is achieved at a phase angle of 105° rather than at the common phase angle of 90° for Gamma type Stirling engine. Pan et al. [141] investigates numerically and experimentally a Vuilleumier (VM) refrigerator (one kind of Stirling refrigerator). The simulation results show that the shuttle loss and regenerator loss are the main factors limiting the performance of VM cryocooler. Results show that the optimal phase angle between hot and cold displacer is about 94°, and the optimal length of stainless steel screen is about 40 mm for this crycooler. Chen et al. [142] studied experimentally and theoretically a pneumatic free piston and free displacer Stirling cryocooler design (FPFD). They propose three expressions of phase shifts deduced from thermodynamic equations of piston and displacer. The three equations are expressed as functions of working parameters as follow:

$$\varphi_{pd} = arctan\left(\frac{(\omega_d^2-\omega^2)M_d}{\omega C_d A_e}\right) + arctan\left(\frac{\widetilde{K_p}}{\omega C_{pp}}\right) \quad (16)$$

$$\varphi_{pp} = arctan\left(\frac{\omega C_{mp}X_p - F_e sin\gamma}{(k_{mp}-\omega^2 M_P)X_p - F_e cos\gamma}\right) \quad (17)$$

$$\varphi_{dd} = arctan\left(\frac{k_{md}-\omega^2 M_d}{\omega C_{md}}\right) = arctan\left(\frac{(\omega_d^2-\omega^2)M_d}{\omega C_{md}}\right) \quad (18)$$

where φ is the displacement phase angle. M_d and M_p are respectively the displacer and the power piston masses. K_p is the stiffness of gas spring in compression space. C_d, C_{pp}, C_{mp}, C_{md} are respectively damping coefficients.ω is the angular frequency. F_e is the force amplitude at the expansion space and γ is the phase shift between the force and electric current.

(c) Dead volume

In practice, volumes other than those scanned by the pistons are called dead volumes. The volumes of the three heat exchangers volumes and of the connecting pipes and the residual volumes of the chambers at the piston end, represent more than 50% of total volume. Dead volume is an essential factor in Stirling engines design, where it should be small as possible. Researches focus on the effect of dead volumes at different SE configurations. Tlili et al. [143] investigates numerically the Yoke Ross SE mechanical output power at different dead volume. It is shown that the dead volumes greatly reduce the SE mechanical output power. The specific power produced is a decreasing function of the dead volume. The dead volume holds in a working fluid proportion which does not accomplish the cycle and therefore does not contribute to the output power. The total dead volume in the Stirling engine represents approximately 58% of the total volume [88].

The needle piston can be a response to the problem of dead volumes. This piston head allows a significant reduction of the dead volumes but the realization of its shape is rather complex. Alfarawi et al. [140] investigates a 500 W Gamma-type SE (Fig. 12). Their results show that the dead volume (connecting pipe) pose negative effects on engine indicated power and therefore, an optimum value of pipe diameter of14 mm were found. Duan et al. [124] purposed Multi-objective Particle Swarm Optimization (MPSO) method to increase SE performances by considering some operating conditions and heat exchanger dead volumes as decision variables. The dead volume increase as well as the heat transfer area decrease destroys SE performances. A compromise is expected between dead volume and heat transfer area of all heat exchangers. The dead volume can be reduced until a minimum volume so that it does not affect heat transfer quantities in each heat exchanger . Based on optimization study and CFD analysis, Xiao et al. redesigned SE heat exchangers in order to decrease dead volume. The proposed optimization model suggests a Stirling engine design of an output power of 270–290 W and a thermal efficiency of more than 18%, whereas the parent engine was of less than 200 W in output power and 16.4% in thermal efficiency. This is mainly due to significant reduction in dead volumes of heat exchangers .

(d) Swept volume

“Swept volume” is defined as the volume of fluid through which a piston or plunger moves when it makes a stroke in an engine. The amount of working gas moving forwards and backwards between the expansion and compression chambers increases with displacer swept volume. Which promotes convective heat transfer between hot and cold ends. Thus, the temperature level in the expansion chamber becomes lower, and that in the compression chamber becomes higher [138]. Tlili et al. [143] illustrates the evolution of output power vs. swept volume. It is shown that the power increases when the swept volume increases until an optimal value. Zhu et al [82] has shown that there is an optimum swept volume ratio of displacer over compressor for efficiency. Kato et al. [96] has shown that a longer displacer stroke increases the indicated work to some extent, although a shorter stroke yields a higher ensemble-average temperature for a hot side displacer chamber. In a Beta type Stirling refrigerator, Hachem et al. [177] has shown that in

Table 9
Different multi-objective optimization recent studies from literature.

Reference (Authors)	Optimization tool	Objective functions	Decision variables
Duan et al. [124]	PSO	Power output, thermal efficiency, and the cycle irreversibility parameter.	Working fluid temperature in the cold space, Working fluid temperature in the hot space, Total dead volume, Expansion volume, Compression volume, Effectiveness of regenerator, Hot space dead volume ratio, Regenerator dead volume ratio, Cold space dead volume ratio, System charge pressure.
Kraitong and Mahkamov [131]	GA	Output power	bores and strokes of the power and displacer pistons
Ahmadi et al. [132]	Non-dominated Sorting Genetic Algorithm (NSGA)	Three objective functions: maximization of output power and efficiency, minimization of total pressure losses	Eleven decision variables : Engine's rotation speed, Mean effective pressure, Stroke, Temperature of heat source, Temperature of heat sink, Temperature difference between heat source and working fluid, Temperature difference between heat sink and working fluid, Number of gauzes of the matrix, Piston Diameter, Regenerator Diameter and length.
Toghyani et al. [108]	Second version of non-dominated sorting genetic algorithm (NSGA-II)	– Maximization of efficiency and output power – minimization of pressure drop	temperature of heat source, stroke, mean effective pressure, and the engine frequency
Duan et al. [124]	PSO (particle swarm optimization)	optimization of power output, thermal efficiency and the cycle irreversibility parameter	temperatures of the working fluid both in the high temperature isothermal process and in the low temperature isothermal process, dead volume ratios of each heat exchanger, volumes of each working spaces, effectiveness of the regenerator, and the system charge pressure.
Patel et al. [135]	TS-TLBO algorithm	Three objective functions simultaneously for the maximization of thermal efficiency, output power and minimization of total pressure drop	Eleven variables: rotation speed, mean effective pressure, stroke length, number of gauzes of the matrix, piston diameter, regenerator diameter, regenerator length, temperature of the heat source, temperature of the heat sink, temperature difference between the heat source and working fluid, temperature difference between heat sink and working fluid.
Luo et al. [136]	parallel multi-algorithms (differential evolution (DE), genetic algorithm (GA) and adaptive simulated annealing (ASA))	–Maximization of thermal efficiency and output power –Minimization of power loss	Frequency, heat source temperature, mean pressure, number of wires and wire diameter of regenerator matrix.
Arora et al. [137]	second version of non-dominated sorting genetic algorithm (NSGA-II)	–power output –thermal efficiency –thermo-economic function	Effectiveness of source-side heat exchanger, effectiveness of sink-side heat exchanger, effectiveness of regenerator, heat source temperature, temperature of working fluid, sink side temperature of the working fluid.
Gheith et al. [116]	Experimental design methodology	–Maximization of output power and efficiency	Four variables: The heating temperature, the charge pressure, the cooling water flow rate and the rotational speed

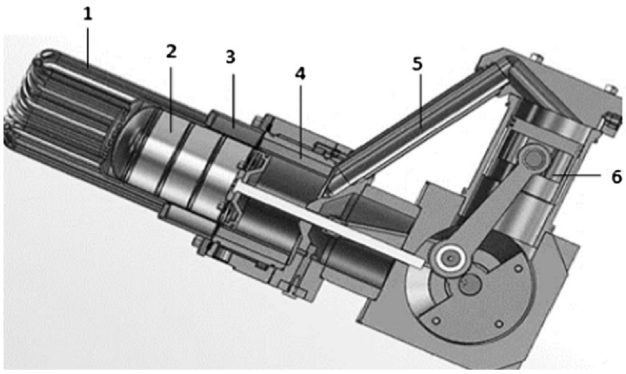

Fig. 12. Engine components: 1-Heater, 2-Displacer piston, 3-Regenerator, 4-Cooler, 5-Connecting pipe, 6-Power piston. (reprinted from Alfarawi et al. [140], copyright 2016 from Elsevier).

order to reach cold temperatures, it is recommended to increase the swept volume of the cold chamber and to reduce its dead volume.

5.2.3.2. Operating parameters.

(a) Temperature ratio

Hot end temperature increase will bring an additional amount of heat to the engine. In fact, the engine resistibility against external load is enhanced at high heating temperature [20]. Consequently the amount of heat giving to the working fluid inside the heater will increase and the heater efficiency too. So the difference of temperature between both working spaces increases and enhances the SE performances. Hot end temperature increase is limited by the working fluid heat capacity. Walker experiments [1] show that the SE mechanical output power depends on the expansion hot temperature. The dimensionless output power increases gradually with the expansion hot chamber temperature. Gheith et al. [23] proved that the SE power and torque increase with hot source temperature. Shuttle loss rises with temperature difference between the two ends of the displacer which is related to temperature gradient between the two heat sources. Sowale et al. [187] concluded that the performance of the Stirling engine is very sensitive to the heat transfer by conduction and the temperature of the working gas.

(b) Frequency or engine speed

The engine rotation speed is a critical parameter for the output brake power and efficiency. The numerical investigation of 500 W Gamma type Stirling engine [97] showed that the evolution of output brake power versus rotation speed reaches an optimal value. In fact, the rotation speed increase reduces heat loss by external conduction through engine's walls, reduces heat exchange time and increases friction loss inside each heat exchanger [97]. This result is approved by Karabulut [119] when investigating the performances of a Beta type Stirling engine driving mechanism by means of a lever. Cheng et al.

Table 10
Regenerator parameters effect from literature.

Parameter(s)	Auteur	Research Focus
Metal material	Hofacker et al. [147]	Identified the best materials used as a regenerator in a Stirling engine, classifying them according to their thermal conductivity and thermal capacity. Graphite was used for the first time as a regenerator. Graphite can exchange twice the amount of heat exchanged with the conventional materials used as regenerator in Stirling engines
	Abduljalil et al. [111]	Identify a low-cost material such as regenerator with performance similar to those of the materials typically used. The cellular ceramics may offer an alternative to traditional regenerator materials to reduce the overall system costs
	Gheith et al. [148]	Four matrices made of different materials have been experimented as regenerator. These materials are: Stainless Steel, Copper, Aluminum and Monel 400 as shown in Fig. 12 (a). The experimental results show that the regenerator Monel 400 stainless steel and Copper has the best thermal efficiency and engine brake power but the presence of oxygen in the working fluid has a great handicap leading to the rapid oxidation of the material, and after the modification of the matrix thermo-physical properties. This degrades extremely heat exchange, and therefore the SE mechanical output power
	Alfarawi et al. [149]	The matrix material of channel regenerator can have strong impact on regenerator performance. The results showed that higher indicated power was obtained using Monel 400 and Stainless steel, while copper has the lowest indicated power. In terms of the cooling power rejected from the engine, ceramic (ZrO_2) and Monel 400 had the lowest cooling power while copper had the highest. This proves that the best regenerator material should have a reasonable volumetric heat capacity and a lower thermal conductivity
Porosity	Timoumi et al. [17,150]	Mesh porosity reduction leads to the highest friction factor and pressure drop. In spite of the higher pressure drop we have better power and thermal efficiency because we have better heat transfer.
	Costa et al. [151]	Performed a numerical simulation for a porosity ranging from 52% to 72% and for Reynolds number ranging from 5 to 50 in the laminar flow regime to investigate the effects of porosity and Reynolds number on pressure drop. In the range of Reynolds number investigated, it is observed that the friction factor obtained from the volumetric porosity of 72% is the highest, followed by the matrix with a volumetric porosity of 64%. But they consider laminar flow through the regenerator wire mesh matrix and Darcy's law to determine the equivalent porous media model
	Gheith et al. [152]	The experimentation of different stainless porosities shows that a porosity of 85% presents the maximal brake power and engine efficiency
Design	Andersen et al. [153]	Propose a new regenerator matrix design. This new design improves engine efficiency from 32.9% to 33.2%. when analyzing numerically a 9KW beta type SE
	Chen et al. [154]	A twin power piston Gamma-type SE was constructed. The engine was incorporated with a moving regenerator housed inside its displacer and filled with a woven-screen material. The effects of different regenerator parameters on engine performance, including regenerator material, wire diameter, mean factor and stacking arrangements, were investigated. According to their results, copper material was found superior to stainless steel on engine performance at the tested conditions and optimum mean factor was proposed
	Nam and Jeong [155]	A parallel wire type regenerator was developed. The friction factor was found to be 20–30% lower than the screen mesh regenerator, but the thermal performance of this new type was poor compared to the screen mesh type due to large axial conduction of parallel wires. The axial conduction losses were further alleviated by the segmentation of the continuous wires but the number of segmentation was limited due to the increased number of housings required to hold the wires
	Bin Wan [156]	Carbon fiber is used as regenerator in SE. it has the characteristics of high temperature resistance, high thermal conductivity and corrosion resistance and using the mean type. The manufacturing costs are very low with long service life and the contact area between the air and the carbon fiber body is large. So the heat transfer efficiency is high
Temperature distribution	Dietrich [157]	–investigates temperature inhomogeneity around the circumference of the regenerator in a Stirling pulse tube (PTC),
	Gheith et al. [116]	–The asymmetry of temperature between both regenerator sides consumes a part of the exchanged thermal energy. The nonsymmetrical design of Gamma Stirling engine is the principal causes of the thermal energy dissipation –An experimental design was proposed for a multi- objective optimization. The choosing Criteria are to maximize the engine power and to minimize the difference of temperature between both regenerator sides. A maximal power of 260 W and a difference temperature of 20 °C are the optimal obtained responses
	Kato et al. [158]	–The regenerator efficiency depends on the working fluid temperature difference between hot and cold chambers and on the pressure fluctuation during a cycle
Length	Xiao et al. [164]	–Pressure drop per unit length decreases as the length of regenerator increases
Design	Tao et al. [160]	–Determine the anisotropic characteristics of a porous medium as regenerator for a cryogenic cooling system (PTR)

[34] developed a dynamic model incorporated with thermodynamic model to study the thermal-lag Stirling engine start process. They found that the optimal engine speed leading to maximum shaft power is significantly influenced by the geometrical parameters (bore size, stroke, and volume of working spaces). According to Chen et al. [138] engine speed pose strong positive effects on power but exert weak effects on efficiency. Optimal frequency depends on the Stirling engine geometric parameters. Dang et al. [145] investigates numerically effects of compressor geometrical parameters on the performances of Stirling pulse tube cryocooler. From their study, they found that adjusting the piston diameter is an effective approach to change the optimal operating frequency. Hachem et al. [177] studied numerically a Beta type Stirling refrigerator using air as working fluid. Their results show that the optimal speed corresponding to the maximum COP is different from its corresponding to the maximum cooling capacity. The maximum can be explained as a compromise between losses that disfavor high heating rate, and losses that disfavor high cooling rates.

(c) Mean pressure

The mean pressure is imposed to the engine before it start-up. It represents the amount of working gas flowing within the engine. This mass is proportional to the initial mean pressure increase. The hot end temperature determines the amount of heat absorbed by the working fluid. The amount of thermal energy exchanged in the engine is closely related to the working gas mass and its corresponding temperature (hot end temperature) [97]. Gheith et al. [146] has shown that the heat exchanged in the heater increases with the initial mean pressure until an optimum value. The regenerator thermal irreversibility decreases with the initial mean pressure. However, the Stirling engine output power and efficiency are enhanced until an optimum value. This assertion is made by Karabulut et al. [119] too. The mean pressure thus has a positive effect on the SE performances up to a limit value after which it becomes negative. At higher values of working fluid mass, work generation becomes lower. Because up and down limits of the working fluid temperature approach to each other [119]. According to the experimental investigations of the Viebach prototype, presented in Ref. [23], the Stirling engine can operate without an initial mean over pressure and can deliver around 69.84 W of brake power. Yang and Cheng [36] showed that the Thermal Lag Stirling Engine could be aself-

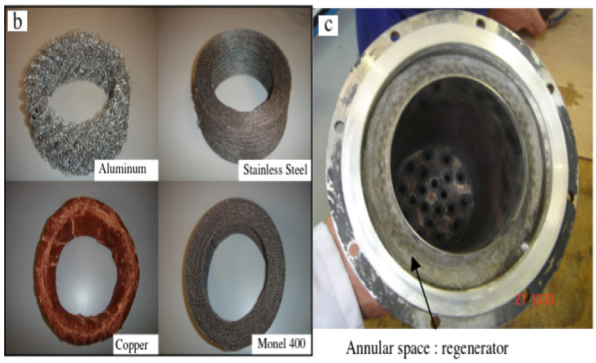

(a) Constituting material of annular regenerator in Gamma type Stirling engine (reprinted from Gheith et al. [152], copyright 2015 from Elsevier).

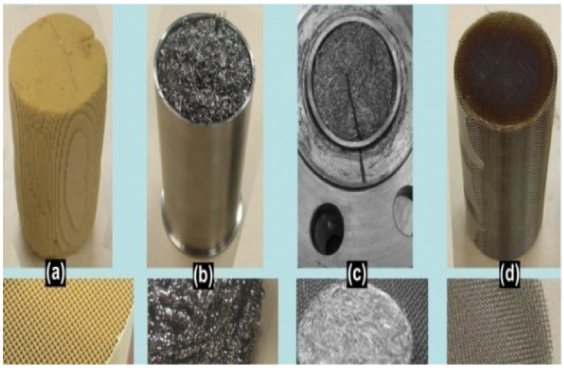

(b) Constituting material of cylindrical regenerator used in thermoacoustic SE (a) Ceramic catalyst support; (b) steel ''scourers''; (c) stainless steel ''wool'' and (d) wire mesh screens. (reprinted from abduljalil et al. [111], copyright 2011 from Elsevier).

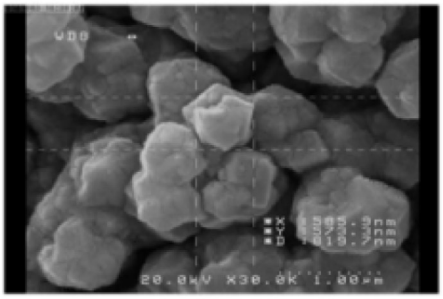

(c) SEM image of matrix surface in metfoam regenerator (reprinted from amel et al. [193], copyright 2018)

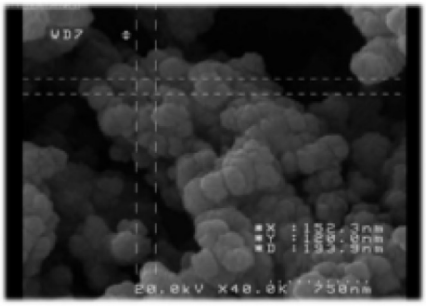

(d) SEM image of matrix surface in nano metfoam regenerator (reprinted from amel et al. [193], copyright 2018)

Fig. 13. Different designs of Stirling engine regenerators.

started engine. And it could be started automatically after applying heating to it. However, it is not possible to start the engine at an atmospheric pressure. Thus, another type of loss named the starting loss can be added to approach the theoretical value to the optimal one.

The three parameters (rotation speed, initial mean pressure and hot end temperature) are dependent and their interactions affect significantly the Stirling engine brake power. The brake power is more sensitive to a change in rotation speed and hot temperature for high initial mean pressure values than for lower values [97].

(d) Oscillating flows characteristics

The flow characteristics of an oscillating flow including porous media are very important for designing Stirling machines [189]. To understand the fundamental characteristics of oscillating flow and heat transfer in a cylinder with a piston partially filled with a porous medium, some research has been done. Khodadadi [190] studied numerically an oscillating flow through a porous channel bounded by two impermeable parallel plates. The author has reported that a better increase in effective heat transfer can be achieved in a field partially filled with a porous medium. Kurzweg et al. [191–193] assumed that heat transfer increased during oscillating flow in a cylinder. Their results showed that, in the case of oscillating flow, the effective diffusivity of heat reaches a maximum for a specific oscillation frequency. Siegel and Perlmutter [194] demonstrated the explicit dependence of heat transfer and frequency. Their results emphasized the importance of the interaction between flow velocity and temperature oscillations, leading to an increase of heat transfer. Lambert et al. [195] have shown that the heat effective diffusion increases during oscillating flow, whatever the nature of the fluid. Recently Ni et al. [189] describes flow characteristics of an oscillating flow including porous media, which is expected to improve the design of Stirling machines. The pressure drop of porous media affects the flows inside the regenerator and other heat exchangers between cylinder and porous media. Thus, they proposed a correlation equation to calculate the cycle-averaged friction factor of porous media. Xiao et al. [196] found that the oscillating flow can share the same correlation equations of steady flow for friction factor within the measured kinetic Reynolds number range and dimensionless fluid displacement. They also found that the effect of gas compression can't be ignored for the steady and oscillating flows through a regenerator with the increase of mass flow, and the pressure drop per unit length decreases as the length of regenerator increases.

5.2.3.3. Heat exchangers parameters. The efficiencies of cooler heater and regenerator are considered as one of the most influential factors amplifying the engine's brake power and efficiency. The output brake power as the engine Carnot efficiency increase with all heat exchangers efficiencies [97].

(a) Regenerator

Stirling engine regenerators are very complex to modeling and designing. It will require a large number of equations to describe their thermodynamic operation. Since it's a balancing act of several factors, some researchers have proposed the best regenerator qualities allowing optimal Stirling engine performances. The engine performances are more sensitive to a change in the regenerator efficiency and its ability to accommodate the high heat flow. The regenerator efficiency increase leads to an increase of the exchanged thermal energy throw it and consequently an amelioration of engine brake power [97]. Tlili et al.

(a) Tubular heater coupled to a biomass boiler in 35kW SE (reprinted from Obernberger et al. [4], copyright 2011).

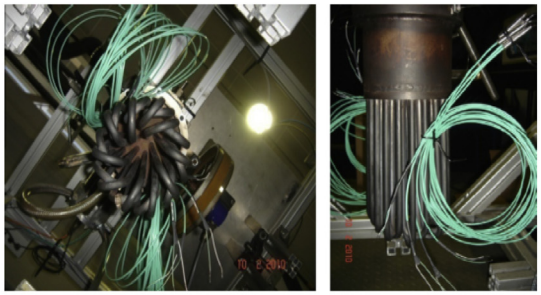

(b) Tubular heater used in 500W Gamma type SE (reprinted from Gheith et al. [150], copyright 2015 from Elsevier).

(c) Finned heater in 1kW double acting SE used in Whispergen boiler (reprinted from Pradip thesis[170], copyright 2016)

(d) Finned cooler in 7kW Gamma-type SE (reprinted from Alfarawi et al.[140],copyright 2016 from Elsevier).

(e) A ceramic heater(reprinted from Akazawa et al. [168]Copyright © by ISEC 2014)

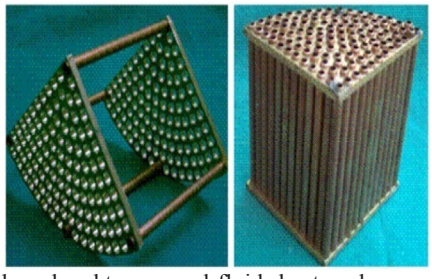

(f) elbow-bend transposed-fluids heat exchanger (El-Ehwany et al. [18] copyright 2011 from Elsevier)

Fig. 14. Different heater designs from literature.

[32] showed that the energy lost in the regenerator represents 86% of the total energy lost in the engine. Hachem et al. [97] showed that the regenerator is the set of 44% of viscous loss, 33% of internal conduction loss and 22% of imperfection loss respectively from the total losses inside a Stirling engine. Compared to Ericsson engine, at nearly the same working conditions, the Stirling engine presents higher specific indicated work and efficiency due to the presence of the regenerator [11]. Many numerical and experimental studies (Table 10) had been performed for the fluid flow and heat transfer performances of different regenerator metal material, mesh size, porosity, dimensions and design.

The constituting material has a direct influence on the efficiency of the regenerator to store heat. Different materials are used as regenerator material such as stainless steel, cooper, aluminum, Monel, graphite, ceramic, Carbon fiber, etc (see Fig. 13). Many researches are made in order to identify the best regenerator material [185] such as Hofacker et al. [147], Gheith et al. [148], Alfarawi et al. [149] and others as shown in Table 10. Clearman et al. [197] experimented several types of annular porous matrices to confirm the importance of the anisotropy and the average pressure in such structures. They tested 5 porous structures: stacked 325 mesh screens, 400 mesh stacked screens, 400 mesh sintered screens, metal foam, alignment of micro-machined nickel discs of 36–40 μm hole diameter. Recently, Amel et al. [188] experimentally investigates the performance of micro and nano metfoam regenerators in alpha-type Stirling engine conditions. Results show an improvement in regenerator percentage of heat recovery by 3.40% and 5.93%, respectively, for micro metfoam and nano metfoam. The maximum improvement is achieved up to 8.65% in case of using the nano metfoam regenerator at 543 K.

(b) Heater and cooler

Hot and cold heat exchangers represent a primordial part in Stirling engines (see Fig. 14). Several Research works had been performed for fluid flow and heat transfer performances of different hot and cold heat exchangers characteristics. Their contribution on ameliorating the Stirling engine output power and efficiency was investigated at different working conditions. Some results are reported in Table 11.

5.2.3.4. Working fluid. Knowing that to achieve a high output power of the Stirling engine, it is preferable firstly to work under high pressure

Table 11
Heater and cooler investigations from literature.

Parameters		Reference (authors)	year	Research Focus
Heat exchange area		Martaj et al. [161]	2006	–The SE mechanical output power depends on the ratio of the exchange area of the cooler A_c to the total exchange area A_t. -Extreme values of the exchange surfaces ratio ($A_c/A_t < 0.2$ or $A_c/A_t > 0.8$) leads to a significant drop in engine performance
Material characteristics		Altamirano et al. [162]	2014	–The SE perform well when the hot heat exchanger has the largest possible heat transfer capabilities, whilst the cold heat transfer capabilities should be limited to an optimal value. –The SE performances can be improved by enhancing and optimizing the heat transfer in the piston chamber
		Akazawa et al. [163]	2014	–A ceramic material (SiC) was proposed as the heater, for 400 W Beta type SE working with helium under 2.5 MPa and 37 Hz, to increase the input heat without heat damage. Results show that the heater efficiency is 63%, the indicated efficiency is 32% and the power output is 389 W. When using a ceramic heater, no cracks and fractures come out even if under 950 °C
Design	flat-shaped heat exchangers or channel-shaped heat exchangers	Kato [175]	2017	–The temperature difference between the two heat exchangers in cases using flat-shaped heat exchangers was 0.08–0.09, that in cases using channel-shaped heat exchangers was 0.10–0.17, and that in case using channel-shaped heat exchangers and regenerators was 0.21
	Tubular heat exchanger	Tlili et al. [43]	2008	–The variation of heater tube diameter can be derived as a function of friction losses for several values of engine speeds. In order to achieve a high effectiveness for the heater and the cooler, larger transfer areas, and thus larger volumes, are needed
		Gheith et al. [146]	2015	–The amount of heat exchanged in the heater increase at lower frequencies. Beyond critical frequency value, the exchange process in the engine proceeds very rapidly, the residence time of the working fluid in the heater is cut short and heat exchanges are deteriorated.
	Non-tubular heat exchanger	García et al. [164]	2012	–The correlations for the friction factor and Stanton number under steady flow conditions is determined to analyze the heater feasibility. These heat exchangers reach high Reynolds numbers and that encounter practical problems associated with the use of bundles of tubes
	Elbow-bend heat exchangers	El-Ehwany et al. [18]	2011	–The elbow-bend heat exchangers having straight tubes are easy to manufacture, have long life time, reliable, light weight and quite cheap to be suitable candidates in Stirling engines compared with the conventional heat exchangers having curved tubes. Elbow-bend heat exchangers reduce the hydraulic losses however they slightly increase the dead volume. Moreover, they can be used for different types of Stirling engines

Table 12
Proprieties of common Stirling engine working fluids.

Working fluid	Thermal conductivity ($W{\cdot}kg^{-1}{\cdot}K^{-1}$)	Specific heat ($kJ{\cdot}kg^{-1}{\cdot}K^{-1}$)	Viscosity ($Pa{\cdot}s$)
Hydrogen	0.1805	14.32	0.0088
Helium	0.1513	5.19	0.0190
Nitrogen	0.02583	1.04	0.0178
Air	0.0239	1.01	0.0183

and secondly to use a working fluid other than air. In this case several research projects (Table 13) determine the effect of working gas (nitrogen, helium, hydrogen or other) on the Stirling engine mechanical output power or on the Stirling refrigerator cooling power. Characteristics of different working fluids usually used in the Stirling engine (hydrogen, helium, air, carbon dioxide) were given in Table 12. Hydrogen provides the greatest amount of heat exchanged and air provides the smallest one. However, Hydrogen presents risks of inflammation. So, it is used only at low and moderate mean pressure. Thus, Helium is thus more advantageous over other gases in high pressurized engines. Differents working fluids are used in Stirling engines even for Stirling generators and Stirling coolers.

6. Conclusion

A detailed literature review of the research efforts made on Stirling generators and Stirling refrigerators has been performed. The aim is to provide comprehensive information about these machines. Current optimizations criterions, methods and parameters for the Stirling machine have been reported. Based on the reviewed technological details it is concluded that:

- The variety of SE applications ensures that the Stirling technology is competitive with conventional power supply. However, there is still a lack of study which explores its cost production.
- The great variety of configurations represents a barrier against the spread of the Stirling technology.
- Stirling engine performances are derived as function of geometric parameters (swept volumes, dead volumes, heat exchange areas, compression ratio…) for several working conditions (speed, mean pressure, temperature difference and working fluid).
- Between the tree heat exchangers, the regenerator characteristics have the greatest impact on the Stirling engine performances. Its parameters (materiel, porosity and design) must be optimized.
- Functioning parameters (rotation speed, initial filling pressure and hot end temperature) are dependent and their interactions affect significantly the Stirling engine performances.
- The choice of heater and coolers design depends on the application of SE. Tubular heat exchangers are usually used in micro-CHP applications. Channel chapped heat exchangers are attractive for low temperature applications.
- An optimum value of the rotation speed must always be respected to ensure the proper functioning of the Stirling machine (The increase of the rotation speed has double effects. On the one hand, it favors the exchanges of heat by convection and on the other hand, it increases the losses by viscous friction through the singularities of the machine).
- The increase of initial charge pressure leads to an increase of working fluid mass, which increases the Stirling engine brake power. However, the load pressure is limited on the one hand by the capacity of the motor to withstand the high pressure (resistance of the materials) and on the other by the realization of a perfect seal (to reduce the leaks of working gas) [185].
- The increase of hot end temperature leads to an increase of the thermal exchanged energy. Thus, the increase of Stirling engine brake power. However, the temperature of the hot end should be

Table 13
Working fluid investigation in literature.

Reference (Authors)	Year	Machine type	Working fluids	Research Focus
Otaka et al. [166]	2002	100 W Beta type Stirling machine	Nitrogen Helium	From their results, they found that the refrigeration produced by nitrogen was 28% less than that produced by helium
Le'an et al. [10]	2009	V-type Stirling Refrigerator (VSR)	Nitrogen Helium	–The rotation speed corresponding to the optimum cooling power depends on the working fluid used either nitrogen or helium. –The optimum COP is about 600 rpm for nitrogen and about 900 rpm for helium
Tekin et al. [167]	2010	V-type Stirling Refrigerator (VSR)	Hydrogen Air Helium	–When the hydrogen is used as the working fluid, the COP of the VSR is higher than the VSR that uses helium or air. This is due to low pressure drop and high specific heat of the hydrogen –The VSR cooling loads are respectively 662, 653 and 624 W respectively when hydrogen, helium and air are used for the working fluid, at a rotation speed 1400 rpm
Chen et al. [168]	2015	Thermoacoustic Stirling heat engine (TASHE)	Nitrogen Argon Helium	–The engine worked with helium in a much wider range of mean pressure than with nitrogen and argon –There was an optimal mean pressure for the minimum onset temperature for each working fluid. The achieved minimal onset temperature differences for argon, helium and nitrogen were 525 °C at 0.51 MPa, 470 °C at 1.1 MPa and 454 °C at 0.35 MPa –The estimated operating frequencies for the three tested working gases were 40 Hz for argon, 44 Hz for nitrogen and 127 Hz for helium
Ni et al. [169]	2015	Stirling engine with U-shaped tubes heater	helium, nitrogen carbon dioxide.	–Helium was found to have the highest heat transfer coefficient in the heater and the lowest temperature difference. Carbon dioxide, with the greatest volumetric heat capacity, was found to have the highest temperature difference and has the second highest heat transfer coefficient among the three working media
Wang et al. [170]	2016	GPU-3 Stirling engine	Helium Hydrogen	–The SE experimental indicated power is much higher with hydrogen than that with helium (it is 2.31 kW for helium, while it is 3.47 kW for hydrogen.) –The Stirling engine has less loss when using hydrogen as the working gas at any working frequency
Dogan et al. [198]	2018	Duplex Stirling refrigerator	Helium, hydrogen and carbon dioxide	–The overall performance and the design of the duplex Stirling refrigerator are examined analytically for different couples of working fluids and the refrigerants. Among the nine fluid couples, the highest performance is maintained when the He is used on both sides

moderate. It is limited by the melting temperature of the material of the hot heat exchanger [185].

- In Stirling engines, the lubrication generates negative effects by creating a lubricant layer over heat transfer surfaces of heater, regenerator and cooler. That is why, the training system should be designed so as to work with a little lubrication or totally dry.
- Working gas leakage is a major difficulty since the engine operates under high pressure.
- The Stirling engine is exposed to continuous internal and external perturbations while operating. However, it cannot change speed quickly.

The need of reducing the fossil fuels use; the need of reducing energy bills, the need of searching alternative ways to produce cleaner energy and the possibility of waste heat recovery encourages us to gain from Stirling engine benefits. Stirling technology fulfils a number of application especially solar applications, micro-CHP applications and cryogenic applications. The Stirling engine has a high potential but there are still some challenges to overcome. Presently, the Stirling technology encounter some limitations namely the controlling difficulty, the problem of gas leakage, thermal and mechanical losses that decreases the Stirling engine performances and the expensive price of the technology. As a conclusion, future research must be carried out and an additional development is needed to produce a practical engine by selection of suitable configuration; adoption of good working fluid; minimization of losses and development of an efficient control system.

References

[1] Walker G, Fauvel R, Gustafson R, van Bentham J. Stirling engine heat pumps. Refrigeration 1982;5(2):91–7.
[2] Martini WR. Stirling engine design manual. University Press of the Pacific. Reprinted from the 1983 edition. ISBN: 1-4102-1604-7; 2004.
[3] Becker M, Funken KH, Schneider G. Solar thermal energy utilization. German Studies on Technology and Application. vol. 5: Final Reports 1989. http://doi.org/10.1007/978-3-642-52342-7.
[4] Obernberger I, Carlsen H, Biedermann F, State-of-the art and future developments regarding small-scale biomass CHP systems with a special focus on ORC AND Stirling engine technologies. In: International nordic bioenergy conference; 2003.
[5] Richard K. Shaltens. Comparison of stirling engines for use with a 25-kW dish-electric conversion system. (EASA) 18 p Avail: 13TIS.
[6] Schreiber JG. RE-1000 Free-piston stirling engine sensitivity test results. NASA TM-88846; 1986.
[7] Urieli I, Berchowitz DM. Stirling cycle analysis. Bristol: Adam Hilger; 1984.
[8] Gras P. Le moteur Stirling et autres moteurs à air chaud une solution aux problèmes énergétiques et environnementaux actuels. Livre; 2010.
[9] Finkelstein T, Polonski C. Development and testing of a stirling cycle machine with characteristics suitable for domestic refrigerators. Report W/M (3A).u.5. Whetstone: English Electric Company Ltd.; 1959.
[10] Le'an S, Yuanyang Z, Liansheng L, Pengcheng S. Performance of a prototype Stirling domestic refrigerator. Appl Therm Eng 2009;29:210–5.
[11] Hachem H, Creyx M, Gheith R, Delacourt E, Morin C, Aloui F, et al. Comparison based on exergetic analyses of two hot air engines: a Gamma type Stirling engine and an open Joule cycle Ericsson engine. Entropy 2015;17:7331–48.
[12] Hachem H, Gheith R, Aloui F, Ben Nasrallah S, Dincer I. Energetic and exergetic performance evaluation of an experimental Stirling machine. Springer book: Progress in Clean Energy, Chapter 55, vol. 2; 2015.
[13] Formosa F, Badel A, Lottin J. Equivalent electrical network model approach applied to a double acting low temperature differential Stirling engine. Energy Convers Manage 2014;78:753–64.
[14] Féniès G, Formosa F, Ramousse J, Badel A. Double acting stirling engine: modeling, experiments and optimization. Appl Energy 2015;159:350–61.
[15] Wu Z, Yu G, Zhang L, Dai W, Luo E. Development of a 3 kW double-acting thermoacoustic Stirling electric generator. Appl Energy 2014;136:866–72.
[16] Costa SC, Barrutia H, Esnaola JA, Tutar M. Numerical study of the pressure drop phenomena in wound woven wire matrix of a Stirling regenerator. Energy Convers Manage 2013;67:57–65.
[17] Timoumi Y, Tlili I, Ben Nasrallah S. Performance optimization of Stirling engines. Renew Energy 2008;33:2134–44.
[18] El-Ehwany AA, Hennes GM, Eid EI, El-Kenany EA. Development of the performance of an alpha-type heat engine by using elbow-bend transposed-fluids heat exchanger as a heater and a cooler. Energy Convers Manage 2011;52:1010–9.
[19] Cheng C-H, Yu Y-J. Dynamic simulation of a beta-type Stirling engine with cam-drive mechanism via the combination of the thermodynamic and dynamic models. Renew Energy 2011;36:714–25.
[20] Hachem H, Gheith R, Aloui F, Ben Nasrallah S, Dincer I. Exergy assessment of heat transfer inside a Beta type Stirling engine. Exergy 2016;20(2):186–201.

[21] Cheng C-H, Huang C-Y and Yang H-S. Experimental and theoretical study of a 90-K beta-type stirling cooler with rhombic-drive mechanism. Copyright © by ISEC International Stirling Engine Committee. All right reserved; 2014.
[22] Cinar C, Yucesu S, Topgul T, Okur M. Beta-type Stirling engine operating at atmospheric pressure. Appl Energy 2005;81(1):351–7.
[23] Gheith R, Aloui F, Tazerout M, Ben Nasrallah S. Experimental investigations of a Gamma Stirling engine. Energy Res 2012;36:1175–82.
[24] Li R, Grosu L, Queiros-Condé D. Losses effect on the performance of a Gamma type Stirling engine. Energy Convers Manage 2016;114:28–37.
[25] Parlak N, Wagner A, Elsner M, Soyhan HS. Thermodynamic analysis of a gamma type Stirling engine in non-ideal adiabatic conditions. Renew Energy 2009;34(1):266–73.
[26] Cheng CH, Yang HS. Optimization of geometrical parameters for Stirling engines based on theoretical analysis. Appl Energy 2012;92:395–405.
[27] Brandhorst HW, Kirby RL, Chapman PA, El-Genk MS. Progress in developing a new 5 kW free-piston Stirling space convertor. AIP conf proc, vol. 969. AIP; 2008. p. 602–8.
[28] Descombes G, Magnet J. (BM 2 593). Moteur non conventionnels . Techniques de l'ingénieur, 1–34.
[29] Lanzetta F. Etude des transferts de chaleur instationnaires au sein d'une machine frigorifique de Stirling. Université de Franche Comte; 1997.
[30] Wang Kai, Sanders Seth R, Dubey Swapnil, Choo Fook Hoong, Duan Fei. Stirling cycle engines for recovering low and moderate temperature heat: a review. Renew Sustain Energy Rev 2016;62:89–108.
[31] Meijer RJ. The Philips hot gas engine with rhombic drive mechanism. Philips Technical Review, vol. 2 (9), chapter 2; 1958.
[32] Tlili I. Étude et modélisation des Moteurs Stirling, [thèse], Ecole Nationale d'Ingénieur de Monastir; 2010.
[33] Tailer Peter L. External combustion otto cycle thermal lag engine. Proceedings of the 28th intersociety energy conversion engineering conference. Atlanta: American Chemical Society; 1993. p. 943–7.
[34] Cheng C-H, Yang H, Jhou B, Chen Y, Wang Y. Dynamic simulation of thermal-lag Stirling engines. Appl Energy 2013;108:466–76.
[36] Yang H-S, Cheng C-H. Theoretical solutions for power output of thermal-lag Stirling engine. Int J Heat Mass Transfer 2017;111:191–200.
[38] Jin T, Huang J, Feng Y, Yang R, Tang K, Radebaugh R. Thermoacoustic prime movers and refrigerators: thermally powered engines without moving components. Energy 2015;93:828–53.
[39] Schmidt G. The theory of Lehmann's calorimetric machine. Zeitschrift Vereines Deutscher Ingenieure 1871;15(1).
[40] Finkelstein T. Insights into the thermodynamics of Stirling cycle machines. AIAA-94-3951-CP; 1994. p. 1829–1834.
[41] Lee FY. Computer simulation of Stirling engines [MSc thesis]. Alberta, Canada: University of Calgary, Calgary; 1976.
[42] Ahmadi MH, Ahmadi M-A, Pourfayaza F. Thermal models for analysis of performance of Stirling engine: a review. Renew Sustain Energy Rev 2017;68:168–84.
[43] Tlili I, Timoumi Y, Ben Nasrallah S. Analysis and design consideration of mean temperature differential Stirling engine for solar application. Renew Energy 2008;33:1911–21.
[44] infinea. 30-kw maintenance-free solar dish engine. DOE Solar Programs Annual Review, Austin, Texas; 2008.
[45] Nepveu F, Ferriere A, Bataille F. Thermal model of a dish/stirling systems. Sol Energy 2009;83(1):81–9.
[46] Hafez AZ, Soliman A, El-Metwally KA, Ismail IM. Design analysis factors and specifications of solar dish technologies for different systems and applications. Renew Sustain Energy Rev 2017;67:1019–36.
[47] Hafez AZ, Soliman A, El-Metwally KA, Ismail IM. Solar parabolic dish Stirling engine system design, simulation, and thermal analysis. Energy Convers Manage 2016;126:60–75.
[48] Kongtragool B, Wongwises S. A review of solar-powered Stirling engines and low temperature differential Stirling engines. Renew Sustain Energy Rev 2003;7:131–54.
[49] http://www.sandia.gov (Sandia, Stirling Energy Systems set new world record for solar-to-grid conversion efficiency).
[50] Yaqi L, Yaling H. Optimization of solar-powered Stirling heat engine with finite-time thermodynamics. Renew Energy 2011;36:421–7.
[51] Grasse W, Hertlein HP, Winter CJ. Thermal solar power plants experience. Plants CJ, Winter RL, Sizmann R, Vant-Hull LL, editors. Solar power Berlin: Springer; 1991. p. 215–82.
[52] Hijazi H, Mokhiamar O, Elsamni O. Mechanical design of a low cost parabolic solar dish concentrator. Alex Eng J 2016;55(1):1–11.
[53] Poullikkas A, Kourtis G, Hadjipaschalis I. Parametric analysis for the installation of solar dish technologies in Mediterranean regions. Renew Sustain Energy Rev 2010;14:2772–83.
[54] Abbas M, Boumeddane B, Said N, Chikouche A. Dish Stirling technology: a 100 MW solar power plant using hydrogen for Algeria. Hydrogen Energy 2011;36:4305–14.
[55] Bakos GC, Antoniades C. Techno-economic appraisal of a dish/stirling solar power plant in Greece based on an innovative solar concentrator formed by elastic film. Renew. Energy 2013;60:446–53.
[56] Barreto Germilly, Canhoto Paulo. Modelling of a Stirling engine with parabolic dish for thermal to electric conversion of solar energy. Energy Convers Manage 2017;132:119–35.
[57] Whispergen.Product specifications. Published online.
[58] CleanEnegy. Gasbox 901 data sheet. Published online.
[59] http://www.microchap.info/stirling_engine.htm.
[60] Barbieri ES, Melino F, Morini M. Influence of the thermal energy storage on the profitability of micro-CHP systems for residential building applications. Appl Energy 2012;97:714–22.
[61] Barbieri ES, Spina PR, Venturini M. Analysis of innovative micro-CHP systems to meet household energy demands. Appl Energy 2012;97:723–33.
[62] De Paepe M, D'Herdt P, Mertens D. Micro-CHP systems for residential applications. Energy Convers Manage 2006;47:3435–46.
[63] Cacabelos A, Eguía P, LuísMíguez J, Rey G, Elena Arce M. Development of an improved dynamic model of a Stirling engine and a performance analysis of a cogeneration plant. Appl Therm Eng 2014;73:608–21.
[64] Conroy G, Duffy A, Ayompe L. Validated dynamic energy model for a Stirling engine m-CHP unit using field trial data from a domestic dwelling. Energy Build 2013;62:18–26.
[65] Parente A, Galletti C, Riccardi J, Schiavetti M, Tognotti L. Experimental and numerical investigation of a micro-CHP flameless unit. Appl Energy 2012;89:203–14.
[66] Creyx M, Delacourt E, Morin C, Desmet B, Peultier P. Energetic optimization of the performances of a hot air engine for micro-CHP systems working with a Joule or an Ericsson cycle. Energy 2013;49:229–39.
[67] Cacabelos A, Eguía P, Míguez JL, Rey G, Arce ME. Development of an improved dynamic model of a Stirling engine and a performance analysis of a cogeneration plant. Appl Therm Eng 2014;73:608–21.
[68] Alfarawi S, Webb-Martin M, Mahmoud S, AL-Dadah RK. Thermal analysis of stirling engine to power automotive alternator using heat from exhaust gases. Energy Procedia 2014;61:2395–8.
[69] Valenti G, Silva P, Fergnani N, Di Marcoberardino G, Campanari S, Macchi E. Experimental and numerical study of a micro-cogeneration Stirling engine for residential applications. Energy Procedia 2014;45:1235–44.
[70] Valenti G, Silva P, Fergnani N, Campanari S, Ravidà A, Di Marcoberardino G, et al. Experimental and numerical study of a micro-cogeneration Stirling unit under diverse conditions of the working fluid. Appl Energy 2015;160:920–9.
[71] Marion M, Louahlia H, Gualous H. Performances of a CHP Stirling system fuelled with glycerol. Renew Energy 2016;86:182–91.
[72] Colmenar-Santos A, Zarzuelo-Puch G, Borge-Diez D, García-Diéguez C. Thermodynamic and exergoeconomic analysis of energy recovery system of biogas from a wastewater treatment plant and use in a Stirling engine. Renew Energy 2016;88:171–84.
[73] Podesser E. Electricity production in rural villages with a biomass Stirling engine. Renew Energy 1999;16:1049–52.
[74] Thiers S, Aoun B, Peuportier B. Experimental characterization, modeling and simulation of a wood pellet micro-combined heat and power unit used as a heat source for a residential building. Energy Build 2010;42(6):896–903.
[75] Huang Yu, Gao Wenzhi, Li Guanghua. Analysis and experiment on exhaust heat recovery of a gasoline engine by a Stirling engine. Copyright © by ISEC International Stirling Engine Committee. All right reserved; 2014.
[76] Arashnia I, Najafi G, Ghobadian B, Yusaf T, Mamat R, Kettner M. Development of micro-scale biomass-fuelled CHP system using Stirling Engine. Energy Procedia 2015;75:1108–13.
[77] Wu Ch. Maximum obtainable specific cooling load of a refrigerator. Energy Convers Manage 1995;36(1):7–10.
[78] Chen L, Xiaoqin Z, Sun F. Cooling load versus COP characteristics for an irreversible air refrigeration cycle. Energy Convers Manage 1998;39:117–25.
[79] Kaushik SC, Tyagi SK, Bose SK, Singhal MK. Performance evaluation of irreversible Stirling and Ericsson heat pump cycles. Therm Sci 2002;41(2):193–200.
[80] He Y-L, Zhang D-W, Yang W-W, Gao F. Numerical analysis on performance and contaminated failures of the miniature split Stirling cryocooler. Cryogenics 2014;59:12–22.
[81] Ataer OE, Karabulut H. Thermodynamic analysis of the V-type Stirling-cycle refrigerator. Refrigeration 2005;28:183–9.
[82] Zhu Shaowei, Nogawa Masafumi. Pulse tube stirling machine with warm gas-driven displacer. Cryogenics 2010;50:320–30.
[83] Tan J, Dang H. An electrical circuit analogy model for analyses and optimizations of the Stirling-type pulse tube cryocooler. Cryogenics 2015;71:18–29.
[84] Caughley A, Sellier M, Gschwendtner M, Tucker A. CFD analysis of a diaphragm free-piston Stirling cryocooler. Cryogenics 2016;79:7–16.
[85] Wang X, Zhu J, Chen S, Dai W, Li K, Pang X, et al. Study on a high capacity two-stage free piston Stirling cryocooler working around 30 K. Cryogenics 2016;80(2):193–8.
[86] Fan S, Li M, Li S, Zhou T, Hu Y, Wu S. Thermodynamic analysis and optimization of a Stirling cycle for lunar surface nuclear power system. Appl Therm Eng 2017;111:60–7.
[87] Hachem H, Gheith R, Aloui F, Ben Nasrallah S. Experimental study of operation stability conditions of a Gamma Stirling engine. In: Proceedings of the ASME 2016 Fluids Engineering Division Summer Meeting, (FEDSM), Washington, DC, USA, July 10–14, 2016.
[88] Beltran-Chacon R, Leal-Chavez D, Sauceda D, Pellegrini-Cervantes M, Borunda M. Design and analysis of a dead volume control for a solar Stirling engine with induction generator. Energy 2015;93:2593–603.
[89] Jaspers HA. Power-control system for Stirling engines. United States: North American Philips Corporation; 1975.
[90] Squier JJDSE. Performance of the vanguard solar Dish-Stirling engine module. Canoga Park, California: Energy Technology Engineering Center; 1986.
[91] Reddy VS, Kaushik SC, Ranjan KR, Tyagi SK. State-of-the-art of solar thermal power plants: a review. Renew Sustain Energy Rev 2013;27:258–73.
[92] Stine WB, Diver RB. A compendium of solar dish/Stirling technology. Other Information: PBD; 1994.
[93] Marks DT. Stirling engine power control and motion conversion mechanism.

Google Patents; 1983.
[94] Simader GR, Krawinkler R, Trnka G. Micro CHP systems: State-of-the-Art, Final Report. Delivrable 8 (D8) of Green Lodges Project (EIE/04/252/S07.38608), Österreichische Energieagentur, Austrian Energy Agency, 2006.
[95] Sauer J, Kuehl H-D. Numerical model for Stirling cycle machines including a differential simulation of the appendix gap. Appl Therm Eng 2017;111:819–33.
[96] Kato Y, Saitoh S, Ishimatsu K, Iwamoto M. Effect of geometry and speed on the temperatures estimated by CFD for an isothermal model of a gamma configuration low temperature differential stirling engine with flat-shaped heat exchangers. Appl Therm Eng 2016.
[97] Hachem H, Gheith R, Aloui F, Ben Nasrallah S. Global numerical characterization of a γ-Stirling engine considering losses and interaction between functioning parameters. Energy Convers Manage 2015;96:532–43.
[98] Cun-quan Z, Cheng Z. Experimental study of a gas clearance phase regulation mechanism for a pneumatically-driven split-Stirling-cycle cryocooler. Cryogenics 2015;66:24–33.
[99] Tlili I. Finite time thermodynamic evaluation of endoreversible Stirling heat engine at maximum power conditions. Renew Sustain Energy Rev 2012;16:2234–41.
[100] Bonnet S. Moteur thermique à apport de chaleur externe étude d'un moteur Stirling et d'un moteur Ericsson [PhD Thesis]. University of Pau et des Pays de l'Adour; 2005.
[101] Araoz Joseph A, Salomon Marianne, Alejo Lucio, Fransson Torsten H. Non-ideal Stirling engine thermodynamic model suitable for the integration into overall energy systems. Appl Therm Eng 2014;73:205–21.
[102] Paul CJ, Engeda A. Modeling a complete Stirling engine. Energy 2015;80:85–97.
[103] Campos MC, Vargas JVC, Ordonez JC. Thermodynamic optimization of a Stirling engine. Energy 2012;44:902–10.
[104] Babaelahi M, Sayyaadi H. Simple-II: a new numerical thermal model for predicting thermal performance of Stirling engines. Energy 2014;69:873–90.
[105] Babaelahi M, Sayyaadi H. A new thermal model based on polytropic numerical simulation of Stirling engines. Appl Energy 2015;141:143–59.
[106] Babaelahi M, Sayyaadi H. Modified PSVL: a second order model for thermal simulation of Stirling engines based on convective–polytropic heat transfer of working spaces. Appl Therm Eng 2015;85:340–55.
[107] Hosseinzade H, Sayyaadi H. CAFS: the Combined Adiabatic-Finite Speed thermal model for simulation and optimization of stirling engines. Energy Convers Manage 2015;91:32–53.
[108] Toghyani S, Kasaeian A, Hashemabadi SH, Salimi M. Multi-objective optimization of GPU3 Stirling engine using third order analysis. Energy Convers Manage 2014;87:521–9.
[109] Gadré I. Price Model of the Stirling Engine. Bachelor of Science Thesis KTH School of Industrial Engineering and Management Energy Technology EGI-2014 SE-100 44 STOCKHOLM.
[110] Ferreira AC, Nunes ML, Teixeira JCF, Martins LASB, Teixeira SFCF. Thermodynamic and economic optimization of a solar-powered Stirling engine for micro-cogeneration purposes. Energy 2016;111:1–17.
[111] Abduljalil Abdulrahman S, Zhibin Yu, Jaworski Artur J. Selection and experimental evaluation of low-cost porous materials for regenerator applications in thermoacoustic engines. Mater Des 2011;32:217–28.
[112] Foster J, Wagner L, and Bratanova A. LCOE models: A comparison of the theoretical frameworks and key assumptions. Energy Economics and Management Group Working Papers 4-2014, School of Economics, University of Queensland, Australia, July 2014.
[113] Levelized cost of energy. (LCOE) metric to characterize solar absorber coatings for the CSP industry. Renew Energy 2016;85:472–83.
[114] Kalogirou S. Solar energy engineering – processes and applications. Elsevier: Academic Press; 2009.
[115] Richard Turton, Bailie Richard C, Whiting Wallace B, Shaeiwitz Joseph A, Bhattacharyya Debangsu. Analysis, synthesis and design of chemical processes. 4th ed. Prentice Hall; 2012.
[116] Gheith R, Aloui F, Ben Nasrallah S. Study of temperature distribution in a Stirling engine regenerator. Energy Convers Manage 2014;88:962–72.
[117] Iwamoto STF. Comparison of low and high temperature differential Stirling engine. In: Proceeding 31st IECEC; 1997. p. 1259–1264.
[118] Formosa F, Despesse G. Analytical model for Stirling cycle machine design. Energy Convers Manage 2010;51:1855–63.
[119] Karabulut H, Cinar C. Torque and power characteristics of a helium charged Stirling engine with a lever controlled displacer driving mechanism. Renew Energy 2010;35:138–43.
[120] Cinar C, Karabulut H. Manufacturing and testing of a gamma type Stirling engine. Renew Energy 2005;30(2):57–66.
[121] Pillet M. Introduction aux plans d'expériences par la méthode Taguchi. Les éditions d'organisations, ISBN 2-7081-1442-5; 1994.
[122] Goupy J. Introduction aux plans d'expériences. Paris: Dunod; 2001. p. 303.
[123] Eberhart R, Kennedy J. A new optimizer using particle swarm theory. In: Proceedings of the 6th international symposium on micro machine and human science, Nagoya, Japan; 1995. p. 39–43.
[124] Duan C, Wang X, Shu S, Jing C, Chang H. Thermodynamic design of Stirling engine using multi-objective particle swarm optimization algorithm. Energy Convers Manage 2014;84:88–96.
[125] Ozgoren YO, Cetinkaya S, Sarıdemir S, Cicek A, Kara F. Predictive modeling of performance of a helium charged Stirling engine using an artificial neural network. Energy Convers Manage 2013;67:357–68.
[126] Tavakolpour-Saleh AR, Zare Sh, Omidvar A. Applying perturbation technique to analysis of a free piston Stirling engine possessing nonlinear springs. Appl Energy 2016;183:526–41.
[127] Ahmadi MH, Ahmadi MA, Sadatsakkak SA, Feidt M. Connectionist intelligent model estimates output power and torque of stirling engine. Renew Sustain Energy Rev 2015;50:871–83.
[128] Zare Sh, Tavakolpour-Saleh AR. Frequency-based design of a free piston Stirling engine using genetic algorithm. Energy 2016;109:466–80.
[129] Audet C, Le Digabel S, Tribes C. NOMAD user guide. Technical Report G-2009-37, Les cahiers du GERAD; 2009.
[130] Srinivas N, Deb K. Muiltiobjective optimization using nondominated sorting in genetic algorithms. Evol Comput 1994;2(3):221–48.
[131] Kraitong Kwanchai, Mahkamov Khamid. Optimisation of low temperature difference Solar Stirling Engines using genetic altorithm. In: Proceedings of the World Renewable Energy Congress – Sweden, 8–13 May, 2011, Linköping, Sweden, vol. 57 (14); 2011. p. 3946–3952. ISSN 1650-3686.
[132] Ahmadi MH, Hosseinzade H, Sayyaadi H, Mohammadi AH, Kimiaghalam F. Application of the multi-objective optimization method for designing a powered Stirling heat engine: design with maximized power, thermal efficiency and minimized pressure loss. Renew Energy 2013;60:313–22.
[133] Ahmadi MH, Mohammadi AH, Dehghani S, Barranco-Jiménez MA. Multi-objective thermodynamic-based optimization of output power of Solar Dish-Stirling engine by implementing an evolutionary algorithm. Energy Convers Manage 2013;75:438–45.
[134] Ahmadi MH, Sayyaadi H, Dehghani S, Hosseinzade H. Designing a solar powered Stirling heat engine based on multiple criteria: Maximized thermal efficiency and power. Energy Convers Manage 2013;75:282–91.
[135] Patel V, Savsani V. Multi-objective optimization of a Stirling heat engine using TS-TLBO (tutorial training and self learning inspired teaching-learning based optimization) algorithm. Energy 2016;95:528–41.
[136] Luo Z, Sultan U, Ni M, Peng H, Shi B, Xiao G. Multi-objective optimization for GPU3 Stirling engine by combining multi-objective algorithms. Renew Energy 2016;94:114–25.
[137] Arora R, Kaushik SC, Kumar R, Arora R. Multi-objective thermo-economic optimization of solar parabolic dish Stirling heat engine with regenerative losses using NSGA-II and decision Making. Electr Power Energy Syst 2016;74:25–35.
[138] Chen W-L, Yang Y-C, Salazar JL. A CFD parametric study on the performance of a low-temperature differential γ-type Stirling engine. Energy Convers Manage 2015;106:635–43.
[139] Erbay LB, Ozturk MM, Dogan B. Overall performance of the duplex Stirling refrigerator. Energy Convers Manage 2017;133:196–203.
[140] Alfarawi S, AL-Dadah R, Mahmoud S. Influence of phase angle and dead volume on gamma-type Stirling engine power using CFD simulation. Energy Convers Manage 2016;124:130–40.
[141] Pan C, Zhang T, Wang J, Zhou Y. Numerical study of a one-stage VM cryocooler operating below 10K. Appl Therm Eng 2016;101:422–31.
[142] Chen X, Wu YN, Zhang H, Chen N. Study on the phase shift characteristic of the pneumatic Stirling cryocooler. Cryogenics 2009;49:120–32.
[143] Tlili I, Musmar SA. Thermodynamic evaluation of a second order simulation for Yoke Ross Stirling engine. Energy Convers Manage 2013;68:149–60.
[144] Xiao G, Sultan U, Ni M, Peng H, Zhou X, Wang S, et al. Design optimization with computational fluid dynamic analysis of b-type Stirling engine. Appl Therm Eng 2017;113:87–102.
[145] Dang H, Zhang L, Tan J. Dynamic and thermodynamic characteristics of the moving-coil linear compressor for the pulse tube cryocooler. Part A: Theoretical analyses and modeling. Refrigeration 2016;69:480–96.
[146] Gheith R, Hachem H, Aloui F, Ben Nasrallah S. Experimental and theoretical investigation of Stirling engine heater : Parametrical optimization. Energy Convers Manage 2015;105:285–93.
[147] Hofacker M, Kong K, Barth EJ. A lumped-parameter dynamic model of a thermal regenerator for free-piston Stirling engines. California, USA: Hollywood; 2009.
[148] Gheith R, Aloui F, Ben Nasrallah S. Determination of adequate regenerator for a Gamma-type Stirling Engine. Appl Energy 2015;139:272–80.
[149] Alfarawi S, AL-Dadah R, Mahmoud S. Potentiality of new miniature-channels Stirling regenerator. Energy Convers Manage 2017;133:264–74.
[150] Timoumi Y, Tlili I, Ben Nasrallah S. Review: Design and performance optimization of GPU-3 Stirling engines. Energy 2008;33:1100–14.
[151] Costa S-C, Tutarb M, Barrenoa I, Esnaolab J-A, Barrutiab H, Garcíad D, et al. Experimental and numerical flow investigation of Stirling engine regenerator. Energy 2014;72:800–12.
[152] Gheith R, Aloui F, Ben Nasrallah S. Study of the regenerator constituting material influence on a gamma type Stirling engine. J Mech Sci Technol 2012;26(4):1251–5.
[153] Andersen SK, Carlsen H, Thomsen PG. Numerical study on optimal Stirling engine regenerator matrix designs taking into account the effects of matrix temperature oscillations. Energy Convers Manage 2006;47:894–908.
[154] Chen W-L, Wong K-L, Chen H-E. An experimental study on the performance of the moving regenerator for a c-type twin power piston Stirling engine. Energy Convers Manage 2014;77:118–28.
[155] Nam K, Jeong S. Development of parallel wire regenerator for cryocoolers. Cryogenics 2006;46(4):278–87.
[156] Wan Bin. Stirling engine regenerator. US 20140331689 A1.
[157] Dietrich M, Yang LW, Thummes G. High-power Stirling-type pulse tube cryocooler: Observation and reduction of regenerator temperature-inhomogeneities. Cryogenics 2007;47:306–14.
[158] Kato Y, Baba K. Empirical estimation of regenerator efficiency for a low temperature differential Stirling engine. Renew Energy 2014;62:285–92.
[159] Xiao G, Peng H, Fan H, Sultan U, Ni M. Characteristics of steady and oscillating flows through regenerator. Heat Mass Transf 2017;108:309–21.

[160] Tao YB, Liu YW, Gao F, Chen XY, He YL. Numerical analysis on pressure drop and heat transfer performance of mesh regenerators used in cryocoolers. Cryogenics 2009;49:497–503.
[161] Martaj N, Grosu L. Exergetical analysis and design optimisation of the Stirling engine. Exergy 2006;3(1):45–66.
[162] Altamirano CF-A, Moldenhauer S, Bayón JG, Verhelst S, De Paepe M. A two control volume model for the Thermal Lag Engine. Energy Convers Manage 2014;78:565–73.
[163] Akazawa T, Hirata K, Hoshino T, Fujiwara K. SiC Ceramics Heater for Free Piston Type of Stirling Engine. Copyright © by ISEC International Stirling Engine Committee. All right reserved.
[164] García D, Prieto JI. A non-tubular Stirling engine heater for a micro solar power unit. Renew Energy 2012;46:127–36.
[165] Pradip PK. Commissioning and Performance Analysis of WhisperGen Stirling Engine. A Thesis. Submitted to the Faculty of Graduate Studies at the university of Windsor, Ontario, Canada; 2016.
[166] Otaka T, Ota M, Murakami K. Study of performance characteristics of a small Stirling refrigerator. Heat Transfer Asian Res 2002;31(5).
[167] Tekin Y, Ataer OE. Performance of V-type Stirling-cycle refrigerator for different working fluids. Refrigeration 2010;33:12–8.
[168] Chen M, Ju YL. Effect of different working gases on the performance of a small thermoacoustic Stirling engine. Refrigeration 2015. http://dx.doi.org/10.1016/j.ijrefrig.2014.12.006.
[169] Ni M, Shi B, Xiao G, Luo Z, Cen K. Heat transfer characteristics of the oscillating flows of different working gases in U-shaped tubes of a Stirling engine. Appl Therm Eng 2015;89:569–77.
[170] Wang K, Dubey S, Choo FH, Duan F. A transient one-dimensional numerical model for kinetic Stirling engine. Appl Energy 2016;183:775–90.
[171] Walker G. Design guidelines for large Stirling cryocoolers. Cryogenics 1983.
[172] Meijer Roelf J. Stirling engines. Saline, Michigan, U.S.A.: Product Innovation Center, Inc.; 2003.
[173] Hachem H, Gheith R, Aloui F, Delprat S, Ben Nasrallah S. Investigation of heat recovery exhaust system of an internal combustion engine coupled to a double acting type Stirling engine. In: International symposium on Sustainable aviation (ISSA), Istanbul, Turkey, 31 May–3 june, 2015.
[174] Thombare DG, Verma SK. Technological development in the Stirling cycle engines. Renew Sustain Energy Rev 2008;12:1–38.
[175] Aliabadi A, Thomson MJ, Wallace JS, Tzanetakis T, Lamont W, Di Carlo J. Efficiency and emissions measurement of a stirling-engine-based residential Micro-cogeneration system run on diesel and biodiesel. Energy Fuels 2009;23:1032–9.
[176] Ust Y, Sahin B, Kodal A. Optimization of a dual cycle cogeneration system based on a new exergetic performance criterion. Appl Energy 2007;84(11):1079–91.
[177] Hachem H, Gheith R, Aloui F, Ben Nasrallah S. Optimization of an air-filled Beta type Stirling refrigerator. Refrigeration 2017;76:296–312.
[178] West CD. Principles and applications of Stirling engines. New York: Van Nostrand; 1986.
[179] Beale WT. Free-piston Stirling engines – some model tests and simulations. In: International automotive engineering congress, Detroit, Paper 690230; 1969.
[180] Organ A. Thermodynamics and gas dynamics of the Stirling cycle machine. Cambridge University Press; 1992.
[181] Altin M, Okur M, Ipci D, Halis S, Karabulut H. Thermodynamic and dynamic analysis of an alpha type stirling engine with scotch yoke mechanism. Energy 2018. http://dx.doi.org/10.1016/j.energy.2018.01.183.
[182] Makhkamov KK, Ingham DB. Analysis of the working process and mechanical losses in a Stirling engine for a solar power unit. ASME J Sol Energy Eng 1999;121:121–7.
[183] Bataineh KM. Numerical thermodynamic model of alpha -type Stirling engine. Case Stud Therm Eng 2018. http://dx.doi.org/10.1016/j.csite.2018.03.010.
[184] Xiao G, Huang Y, Wang S, Peng H, Ni M, Luo Zhongyang, Cen Kefa, Gan Zhihua. An approach to combine the second-order and third-order analysis methods for optimization of a Stirling engine. Energy Convers Manage 2018;165:447–58.
[185] Gheith R, Hachem H, Aloui F, Ben Nasrallah S. Stirling engines. Comprehensive Energy Systems. Elsevier book Chapter 409; 2018.
[186] Mohammadi MA, Jafarian A. CFD simulation to investigate hydrodynamics of oscillating flow in a Beta-type Stirling engine. Energy 2018. http://dx.doi.org/10.1016/j.energy.2018.04.017.
[187] Sowale A, Kolios AJ, Fidalgo B, Somorin T, Parker A, Williams L, et al. Thermodynamic analysis of a gamma type Stirling engine in an energy recovery system. Energy Convers Manage 2018;165:528–40.
[188] Amel AN, Kouravand S, Zarafshan P, Kermani AM, Khashehchi M. Study the heat recovery performance of micro and nano metfoam regenerators in alpha type Stirling engine conditions. Nanoscale Microscale Thermophys Eng 2018. http://dx.doi.org/10.1080/15567265.2018.1456581.
[189] Ni M, Peng H, Sultan U, Luo K, Xiao G. A quantitative method to describe the flow characteristics of an oscillating flow including porous media. Int J Heat Mass Transf 2018;119:860–6.
[190] Khodadadi JM. Oscillatory fluid flow through a porous medium channel bounded by two impermeable parallel plates. J. Fluids Eng. 1991;113:509–11.
[191] Kurzweg UH, Zhao LD. Heat transfer by high frequency oscillations; a new hydrodynamic technique for achieving large effective axial conductivities. Phys Fluids 1984;27:2624–7.
[192] Kurzweg UH. Enhanced heat conduction in fluids subjected to sinusoidal oscillations. J. Heat Transfer 1985;107:459–62.
[193] Kurzweg UH. Enhanced heat conduction in oscillating viscous flows within parallel plate channels. J. Fluid Mech 1985;156:291–300.
[194] Siegel R, Perlmutter M. Heat transfer for pulsating laminar duct flow. Trans. ASME J. Heat Transf 1962;84(2):111–23.
[195] Lambert AA, Cuevas S, del Rio JA, Lopez M. Heat transfer enhancement in oscillatory flows of Newtonian and viscoelastic fluids. Int. J. Mass Transf 2009;52:5472–8.
[196] Xiao G, Peng H, Fan H, Sultan U, Ni M. Characteristics of steady and oscillating flows through regenerator. Int J Heat Mass Transf 2017;108A:309–21.
[197] Clearman WM, Cha JS, Ghiaasiaan SM, Kirkconnell CS. Anisotropic steady-flow hydrodynamic parameters of microporous media applied to pulse tube and Stirling cryocooler regenerators. Cryogenics 2008;48:112–21.
[198] Dogan B, Ozturk MM, Erbay LB. Effect of working fluid on the performance of the Duplex Stirling refrigerator. J Clean Prod 2018. http://dx.doi.org/10.1016/j.jclepro.2018.04.076.
[199] Çinar C, Aksoy F, Solmaz H, Yilmaz E, Uyumaz A. Manufacturing and testing of an a-type Stirling engine. Appl Therm Eng 2018;130:1373–9.
[200] Erol D, Yaman H, Dogan B. A review development of rhombic drive mechanism used in the Stirling Engines. Renew Sustain Energy Rev 2017;78:1044–67.

Further reading

[35] Cheng Chin-Hsiang, Yang Hang-Suin. Theoretical model for predicting thermodynamic behavior of thermal-lag Stirling Engine. Energy 2013;49:218–28.
[37] Yang H-S, Cheng C-H. C-H. Stability analysis of thermal-lag Stirling engines. Appl Therm Eng 2016;106:712–20.